Nonlinear Modeling of Locomotive Propulsion System and Control

Henrik Sandberg

Supervisors:
Andrew Paice,
Anders Rantzer &
Bo Bernhardsson

Department of Automatic Control, Lund Institute of Technology

27th August 1999

Abstract

In this report the motor side of a converter driven AC-locomotive is studied and modeled. The motor side consists of an asynchronous electrical engine, an indirect self controller, a voltage converter, a Pulse Width Modulator(PWM) and the train mechanics. The converter is supplied with voltage from a DC-link. The link is connected to a line converter which transfers energy from the railway net to the link.

The modeling is made in frequency domain with a method allowing frequency interaction. The technique is based on the use of truncated Fourier series. The signals are described with vectors containing the Fourier coefficients. Matrices called Harmonic Transfer Matrices(HTM) are constructed to describe the relation between two such vectors.

In Linear Time Invariant(LTI) systems the HTM:s are diagonal. Linear Time Periodic(LTP) systems on the other hand gives HTM:s with off-diagonal elements. That means an input frequency can generate other frequencies. Nonlinear systems also have this charasteristic, although they cannot be exactly described with HTM:s. For small perturbations around a periodic solution they are often well approximated with a HTM.

In the report HTM:s are developed for each of the motor side components mentioned above. The engine and the controller are nonlinear but are approximated as LTP systems. A HTM is then easy to get. The converter and the PWM are nonlinear and are modeled together. The HTM is obtained analytically by considering changes of switch time points. A simple LTI mechanical model is used.

The engine-controller-mechanics loop is closed and a HTM for the entire system is obtained. With it it is possible to see the spectral changes of motor variables such as stator current and mechanical frequency when the set point of the torque is changed. It is also possible to see the effects of spectral changes of the DC-link voltage on the motor and on the current in the DC-link. The results are compared to `Simulink`-simulations of the system. The agreement is good.

An iterative procedure is also presented to make it possible to connect the motor side HTM with an analog model of the line side. Together they would model the entire locomotive. Such tests are not performed in this report.

Contents

Preface

I would like to take the opportunity to thank ABB Corporate Research Center, Baden-Dättwil, Switzerland, for giving me the opportunity to carry out my master thesis in a very fine and stimulating working environment. I was able to fully concentrate on the subject and got all the help I asked for. Especially I would like to thank my supervisor at the center, Dr. Andrew Paice, with whom I worked on the project. He gave many invaluable ideas and comments to the project and helped me with all the practial issues.

I would like to thank the person behind the project: Dr. Markus Meyer at Adtranz, Oerlikon, Switzerland. He provided with the questions and a great knowledge of locomotives.

I would also like to thank my supervisors at the Department of Automatic Control, Lund Institute of Technology: Dr. Anders Rantzer, Dr. Bo Bernhardsson and Erik Möllerstedt. They supplied me with literature and ideas and introduced me to the modeling technique.

Zürich, 27 August, 1999
Henrik Sandberg

1 Introduction

Most modeling in frequency domain is made on purely linear or linearized systems. In this report an attempt is made to model Linear Time Periodic (LTP) and Nonlinear Systems in the frequency domain. The method is based on truncated Fourier series and leads to a matrix formulation of the problem. It can be viewed as a linearization in frequency domain. The method has been applied to for example switched electrical systems [1] and to general LTP systems [2].

In this report the propulsion system of an AC-locomotive is studied. It is natural to divide the locomotive into two parts: the line and the motor side. In fact the motor side can be viewed as a DC-locomotive. The line side has the task to convert the $16\frac{2}{3}\ Hz$ line alternating voltage (in Switzerland) to direct voltage stored in a link, which feeds the motor voltage converter. Therefore the DC-link could be looked at as a DC-railway network. The motor side consists mainly of three parts: an Asynchronous Electrical Motor (ASM), a motor controller and a voltage converter. These three systems will be modeled separately in the frequency domain based on existing time domain models. They are then put together to obtain a closed loop system.

This model will then be connected to a frequency domain model of the line side. The resulting model can predict the effects of a harmonic perturbation of one or many of the locomotive inputs. For example: if a harmonic perturbation of the set point of the torque is introduced, what is the effect on the current from the net? That is, what frequencies are created and of what magnitude. The models made so far don't take the nonlinearities into account.

The underlying reason for this work is the fact that there have been stability problems of the railway networks in a couple of countries. Some examples:

- Italy: Electrical line disturbances in 1993-1995.
- Denmark: Several protective shutdowns of the net in 1994.
- Great Britain: Problem with signalling systems in 1994-1995.
- Switzerland: Several modern converter locomotives shut down due to network resonance in 1995.
- Germany: S-Bahn in Berlin exceeded the limits for harmonical perturbations in 1995.

As modern locomotives of converter type are responsible for these problems a better understanding of their interaction with the electrical net is needed. There is an international reasearch project named ESCARV (Electrical System Compatibility for Advanced Rail Vehicles), which has as goal to develop methods to test compatibility of railnetworks, locomotives and signalling equipment. All the large train manufacturers in Europe, the Swiss and Italian railway companies and some universities are members in this project. The project should be finished in the end of year 2000. More informtion can be found in [3] and on `www.enotrac.com/escarv`.

1.1 Structure of the Report

In section 2 the mathematical theory will briefly be treated and the symbols used be explained. In section 3 the AC-locomotive is presented. In section 4 the different subsystems of the locomotive are explained and the mathematical models are given. Section 5 presents the approximations and the methods used to construct the frequency domain models. In section 6 some analysis will be made on the frequency domain models and it will be shown how good the results are compared to simulations in time domain. There it also will be shown how to choose an operating point and how to connect the model to line side models. In section 7 are some conclusions made and some suggestions for future work are given. In the appendix MATLAB-code which performs the tasks in the report is included.

2 Theory

In this section the mathematical background of the method used will be given. The study of harmonic interactions of this kind comes mainly from the field of electrical engineering. In the literature you can find quite a lot on this subject under the name *Harmonic Balance*, see for example [4]. But the question of finding a generalized transfer function is also of interest to people doing control theory. For example Linear Time Periodic systems will be treated later, these are often used in modeling and control of helicopters and wind mills.

2.1 Steady State Simulation

In this report all considerations will be made under steady state. This means that all transients have died out and all quantities are constant or periodic. Periodic functions can be expanded into a Fourier series with harmonic functions as basis. In the general case you need an infinite number of frequencies to expand a function, but in computer implementations you have to truncate after a finite number of terms. In practice this is sufficient, as the functions under consideration may often be approximated with just a few harmonics.

Let the periodic function have a fundamental frequency of ω_0 and the corresponding period T. The harmonics might be used in complex form $e^{j\omega_0 t}$ or in real form $\sin\omega_0 t$ and $\cos\omega_0 t$ where $\omega_0 T = 2\pi$. Both representations have their advantages. In this report the complex form will be used most often. The Fourier series then is written as:

$$v(t) = \sum_{k=-\infty}^{\infty} c_k e^{jk\omega_0 t},$$

where

$$c_k = \int_t^{t+T} v(\tau) e^{-jk\omega_0 \tau} d\tau$$

As the goal of this report is to construct a matrix formulation of the system, the function will be represented through the vector

$$\mathcal{V} = [\ \ldots\ \ c_{-2}\ \ c_{-1}\ \ c_0\ \ c_1\ \ c_2\ \ \ldots\ ]^T$$

If the function $v(t)$ is real then $c_{-k} = c_k^*$ where * denotes complex conjugate. This might be used to reduce the number of components. More information about Fourier series can be found in [5] for the mathematical aspects and in [6] for the electrical engineering aspects.

As this report is going to treat harmonical interaction between two functions $v(t)$ and $i(t)$ this must be modeled in some way. To make it simple we choose a linear relationship

$$I = \mathcal{Y}\mathcal{V} \tag{1}$$

where I is the coefficient vector for $i(t)$ and $\mathcal{Y}$ is called a Harmonical Transfer Matrix (HTM). The HTM is the tool to describe the interaction. As matrix multiplication is a linear operation it is still quite simple but it is able to model phenomenons that can't be captured with the normal transfer function when analyzing systems. The coupling between the HTM and the

Laplace transfer function will be given in section 2.2. The HTM has been used in some other reports, for example in [1] and [7].

By having non-diagonal elements in $\mathcal{Y}$ one frequency can produce other frequencies in the output. A couple of different situations are going to be treated in the next sections.

2.2 Linear Time Invariant Systems

In classical linear systems with constant coefficients (LTI) it is a well known fact that a single frequency as input only produce the same frequency as output. The output may have a different amplitude and phase angle. Some examples from electrical engineering are the resistor, the capacitor and the inductor. Their respective time domain relationships are:

$$Ri = v, \;\; C\frac{dv}{dt} = i, \;\; L\frac{di}{dt} = v$$

Where i is the current and v the voltage. As derivatives are linear operators and the multiplications are with constant coefficients these relationships can be rewritten in steady state form (1) where

$$\begin{aligned}
\mathcal{Y}_R &= \text{diag}\{1/R, 1/R, \ldots, 1/R\} \\
\mathcal{Y}_C &= \text{diag}\{-jN\omega_0 C, -j(N-1)\omega_0 C, \ldots, jN\omega_0 C\} \\
\mathcal{Y}_L &= \text{diag}\{-1/jN\omega_0 L, -1/j(N-1)\omega_0 L, \ldots, 1/jN\omega_0 L\}
\end{aligned}$$

The $\mathcal{Y}$:s are HTM:s but as the two time functions are voltage and current they are usually called admittance matrices. As seen it is very comfortable to work with linear expressions in frequency domain. The matrices become purely diagonal.

In the LTI case we have the Laplace transformation $G(s)$ of the system. The fundamental signal of LTI:s are the complex exponential, e^{st}. If a complex exponential is the input to the LTI system then the output also is a complex exponential multiplied with the complex transfer function with the frequency as argument (steady state conditions), see figure 1. Time periodic signals always have $s = j\omega$ so to construct a HTM from the transfer function we have

$$\mathcal{Y} = \text{diag}\{G(-jN\omega_0), G(-j(N-1)\omega_0), \ldots, G(jN\omega_0)\}$$

2.3 Linear Time Periodic Systems

If the linear system have time periodic coefficients the dynamics becomes a bit more involved. Analysis with the Laplace transformation becomes hard to carry through. In order to get a HTM another theory is used. The following is developed according to [2].

A general Linear Time Periodic (LTP) system can be written as

$$\frac{d}{dt}x(t) = A(t)x(t) + B(t)v(t) \tag{2}$$

$$i(t) = C(t)x(t) + D(t)v(t) \tag{3}$$

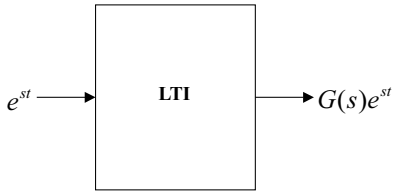

Figure 1: The steady state response of a LTI system to a complex exponential. G is the transfer function.

where $v(t) \in R^n$ is input, $i(t) \in R^m$ is output and $x(t) \in R^o$ is a suitable state vector. $A(t) \in R^{o\times o}, B(t) \in R^{o\times n}, C(t) \in R^{m\times o}, D(t) \in R^{m\times n}$ are time periodic matrices of period T. Such systems have been throughly studied in [2], where a lot of interesting results are given. Here only a few of them are presented and for more detailed proofs this is a good reference.

One result of interest is that Geometrically Periodic signals (GP, see definition below) are to LTP systems what complex exponentials are to LTI systems. That is, if a GP signal is input to a LTP system then the output also is GP.

DEFINITION 1 (Geometrically Periodic Signals)
A geometrically periodic signal $u(t)$, with fundamental frequency ω_0, and corresponding fundamental period T, has the property that

$$u(t + NT) = z^N u(t)$$

where $z \in C$ and $N \in Z$

As a special case of GP signals we have the exponentially modulated periodic signal:

$$u(t) = e^{\lambda t} \sum_{k=-\infty}^{\infty} u_k e^{jk\omega_0 t}$$

where λ is a complex variable. Note that when $\lambda = 0$ it reduces to a normal Fourier series and when $\lambda = j\omega$ it is a convolution of two periodic functions in frequency domain.

Now to construct a HTM between $\mathcal{V}$ and I we expand all quantities in Fourier series where the input, the state and the output vector may be exponentially modulated. That gives:

$$A(t) = \sum_{k=-\infty}^{\infty} A_k e^{jk\omega_0 t}$$

$$x(t) = e^{\lambda t} \sum_{k=-\infty}^{\infty} x_k e^{jk\omega_0 t}$$

$$\frac{d}{dt}x(t) = e^{\lambda t} \sum_{k=-\infty}^{\infty} (\lambda + jk\omega_0) x_k e^{jk\omega_0 t}$$

where A_k are matrices and x_k are column vectors. The other variables are expanded analogously. If this is inserted in eq.(2) and (3) they can be

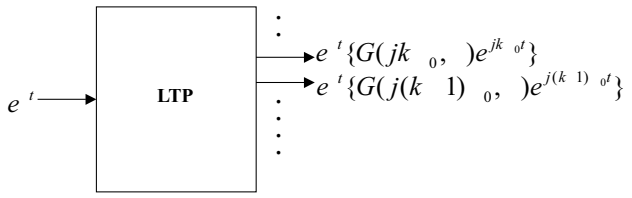

Figure 2: The steady state response of a LTP system to a complex exponential. The input frequency becomes amplitude modulated with the systems time varying frequency, ω_0. In general an infinte amount of frequencies are needed to describe the system. G is a generalized transfer function dependent on the input frequency λ and the modulation frequency ω_0.

rewritten as

$$0 = \sum_{k=-\infty}^{\infty} \left\{ (\lambda + jk\omega_0)x_k - \sum_{l=-\infty}^{\infty} A_{k-l}x_l - \sum_{l=-\infty}^{\infty} B_{k-l}u_l \right\} e^{(\lambda+jk\omega_0)t}$$

$$0 = \sum_{k=-\infty}^{\infty} \left\{ i_k - \sum_{l=-\infty}^{\infty} C_{k-l}x_l - \sum_{l=-\infty}^{\infty} D_{k-l}u_l \right\} e^{(\lambda+jk\omega_0)t}$$

As the complex exponentials form an orthogonal basis in $L_2[0,T]$ must the terms enclosed by braces vanish. Hence for all $k \in Z$ we have

$$(\lambda + jk\omega_0)x_k = \sum_{l=-\infty}^{\infty} A_{k-l}x_l + \sum_{l=-\infty}^{\infty} B_{k-l}u_l$$

$$i_k = \sum_{l=-\infty}^{\infty} C_{k-l}x_l + \sum_{l=-\infty}^{\infty} D_{k-l}u_l$$

These sums can be written as matrix relationsships with the Fourier coefficients as elements:

$$\lambda\mathcal{X} = (\mathcal{A} - \mathcal{N})\mathcal{X} + \mathcal{B}\mathcal{V} \quad (4)$$

$$I = C\mathcal{X} + \mathcal{D}\mathcal{V} \quad (5)$$

where $\mathcal{X}^T = [\ \ldots\ x_{-1}^T\ x_0^T\ x_1^T\ \ldots\ ]$ and similar for $\mathcal{V}$ and I. The time periodic system matrix is written as a doubly infinite Toeplitz matrix

$$\mathcal{A} = \begin{bmatrix} \ddots & \vdots & \vdots & \vdots & \\ \ldots & A_0 & A_{-1} & A_{-2} & \ldots \\ \ldots & A_1 & A_0 & A_{-1} & \ldots \\ \ldots & A_2 & A_1 & A_0 & \ldots \\ & \vdots & \vdots & \vdots & \ddots \end{bmatrix} \quad (6)$$

and similar for $\mathcal{B}, C, \mathcal{D}$. $\mathcal{N}$ finally is a doubly infinite block diagonal matrix containing multiplies of the fundamental frequency ω_0:

$$\mathcal{N} = \text{blkdiag}\{jk\omega_0 I\}, \quad \forall k \in Z$$

We now would like to construct a HTM between $\mathcal{V}$ and I, an admittance matrix in a special case. This is done in exactly the same way as in the LTI case in state space formulation. That means we eliminate $\mathcal{X}$ in eq.(4) and (5). The result is:

$$I = \mathcal{Y}(\lambda)\mathcal{V}$$

where

$$\mathcal{Y}(\lambda) = C[\lambda I - (\mathcal{A} - \mathcal{N})]^{-1}\mathcal{B} + \mathcal{D} \tag{7}$$

Notice when $\lambda = 0$ we have exactly the same matrix as in section 2.2. In the thesis of Wereley a lot of properties of these matrices are shown. By calculating the eigenvalues of $\mathcal{Y}(\lambda)$ for different λ it is possible to make a generalized Nyquist plot and to formulate a stability criterium.

In the coming sections nonlinear systems will be approximated with these LTP systems and the methods above can then be used to construct the desired admittance matrix.

2.4 Nonlinear Systems

In the general nonlinear case it is of course hard to construct a general method. Many times it is interesting to study switched system where the switching action depends on the state of the system. The true relationship between the current and the voltage in the frequency domain looks like:

$$I = F(\mathcal{V})$$

Often F is hard to define explicitly due to switching and other nonlinearities. One approach is to divide the system into a linear part, which is easy to describe, and a nonlinear part. The result is a nonlinear equation system. Such systems can be solved in a number of different ways, for example with fix-point iteration or Newton's method. The problem is that convergence is not guaranteed and that a first guess of a solution must be supplied, which may be hard to find if the number of unknowns is large. Also the nonlinear response to a periodic voltage sometimes must be computed via time domain simulations, which are costly if made every iteration. This treatment is called Harmonic Balance and more details are found in [1] and in [4].

A way to go around the complicated procedure above is to make a linearization of F. The following is developed according to [1]. If a steady state solution , I_0 and $\mathcal{V}_0$, is known this can be used as a linearization point. Around this point the relationship between I and $\mathcal{V}$ approximately can be written as

$$I = I_0 + \mathcal{Y}(\mathcal{V} - \mathcal{V}_0) \tag{8}$$

according to Taylor's theorem where

$$\mathcal{Y} = \frac{\partial I}{\partial \mathcal{V}} = \begin{bmatrix} \frac{\partial C_{-N}}{\partial c_{-N}} & \frac{\partial C_{-N}}{\partial c_{-N+1}} & \cdots & \frac{\partial C_{-N}}{\partial c_N} \\ \frac{\partial C_{-N+1}}{\partial c_{-N}} & \frac{\partial C_{-N+1}}{\partial c_{-N+1}} & \cdots & \frac{\partial C_{-N+1}}{\partial c_N} \\ \vdots & \vdots & \ddots & \vdots \\ \frac{\partial C_N}{\partial c_{-N}} & \frac{\partial C_N}{\partial c_{-N+1}} & \cdots & \frac{\partial C_N}{\partial c_N} \end{bmatrix} \tag{9}$$

Here C_k are the elements of I and c_k are the elements of $\mathcal{V}$. Often though it is more convenient to work with the real representation of the Fourier series when calculating the Jacobian. This is due to the problems with complex derivation which might be hard in real situations.

Thus eq.(9) gives the approximate admittance matrix around the linearization point. The problems here are to find the linearization point and to evaluate the Jacobian (9). These things might be necessary to do through simulations or experiments.

In [1] a HTM of a dimmer is constructed with an analytical linearization procedure. The calculated results are then compared with measurements and simulations with very good agreement. This demonstrates that the method can be used in systems with hard nonlinearities. It is also shown how you can model subsystems in this way and then put all the admittance matrices together to get the frequency response of the entire system. This is called to construct a Norton equivalent.

2.4.1 Convolution

In quite a few cases in this report, the nonlinearities are simple multiplication of two quantities, typically $x(t)$ and $y(t)$. If they both are time periodic with the period T then the Fourier series of their product is a convolution of the two Fourier expansions. This is a well known fact see for example [6].

Assume now each of them are disturbed by $\Delta x(t)$ and $\Delta y(t)$ which also are time periodic. Their product is then well approximated (small perturbations) by:

$$p(t) = x(t)y(t) \approx x_0(t)y_0(t) + y_0(t)\Delta x(t) + x_0(t)\Delta y(t) \tag{10}$$

where $x_0(t)$ and $y_0(t)$ are the beforehand known periodic solutions. The error is here of second order. Note that if the known solution is constant this reduces to a classical linearization, otherwise we have multiplication with time periodic coefficients. This can be written in the frequency domain as:

$$\Delta\mathcal{P} = \mathcal{E}\Delta\mathcal{X} + \mathcal{F}\Delta\mathcal{Y} \tag{11}$$

where $\Delta\mathcal{X}$ and $\Delta\mathcal{Y}$ are the complex Fourier coefficient vectors and $\mathcal{E}$ and $\mathcal{F}$ are Toeplitz matrices just like eq.(6) with the Fourier coefficients of $x_0(t)$ and $y_0(t)$ as elements. This relation also holds when the inputs (perturbations) are exponentially modulated Fourier series like in 2.3. Therefore it can be combined with HTM of the form (7) when $\lambda \neq 0$.

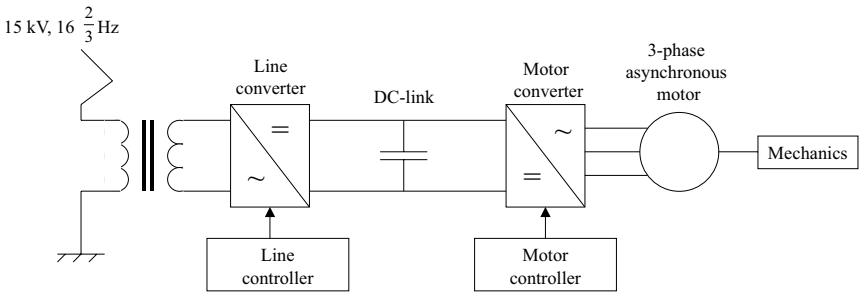

Figure 3: System overview of a converter locomotive.

3 AC-Locomotives

In this report converter AC-locomotives are modeled. Here the locomotive will briefly be described and the advantages and the problems with the technology be told. The locomotive is of general type propulsed by an asynchronous electrical engine fed through voltage converters. As the converters are constructed with GTO(Gate Turn Off)-thyristors, semiconductor switches that can handle high voltages, the technology is quite modern. It was not until the 80's this technology had its breakethrough and became economically efficient. But the new technology also brought some new problems.

A system diagram of a converter locomotive is shown in figure 3. The railway electrical network voltage in Switzerland and in many other countries is 15 kV and of frequency $16\frac{2}{3}$ Hz. In the AC-locomotive this voltage first is transformed down to a minor voltage and then fed to the net side converter. The task of the converter is to make direct current out of the alternating current. This is obtained through a controller which produces switching signals to the converter. The controller measures the frequency of the net, the voltage of the net and the DC-link plus some other quantities. The goal of the controller is to keep a constant DC-link voltage, maintain stability of the DC-link and to draw a sinusoidal current from the net of the same frequency as the main net voltage.

The output voltage of the net side converter is of course not purely DC. The power from the net pulsates with the double net frequency, $33\frac{1}{3}$ Hz. The DC-link is supposed to have a constant voltage so therfore a compensator circuit based on capacitors is added to compensate for exact this frequency. As the input power not always is equal to the motor power another capacitor circuit is added to fill in or store the deficit/surplus power. The DC-link also supplies the transformer with the needed reactive power, this is of utmost importance as reactive power is to be avoided on the railway net. Reactive power from the net leads to unnecessary currents increasing power loss.

In the other end of the DC-link another voltage converter is connected. This converter makes AC out of the DC, this time of variable frequency. The frequency must be variable in order to drive the engine at different speeds and torques. As the dynamics of the engine not is linear the question of producing the right frequency and the right amplitude is not so easy to answer. There are different control strategies in different operating areas.

As the report treats the motor side the motor and these control strategies will be studied in more detail in the next sections.

A simple way of thinking how the locomotive works is to see the DC-link as an energy resevoir. The motor then draws the wanted amount of energy to fullfill the commands from the motor controller. The task of the net controller is then to supply energy to this resevoir by transferring it from the railway net.

As was mentioned in the introduction there have been stability problems in the railway electrical network. The problems in Switzerland occurred when a lot of these converter locomotives were in action and at the same time older locomotives not using converter technology were off-line. The problem turned out to be the interaction of the locomotives with the network. The electrical network covers very large areas which implies the resonance frequency of the net is fairly low. When the net generators are taken into account there is a resonance frequency at about 150 Hz. This is normally not a problem. The resonance is damped by all the passive components in the net (copper losses in transformers and generators, non-converter locomotives and heating of the trains).

The net voltage should be $16\frac{2}{3}$ Hz, but there are higher harmonics in the voltage. The net side controller in the locomotive tries to draw current from the net of the main frequency. However it is inevitable that currents of the higher harmonics are created. If a frequency analysis is made on the locomotive it shows that in the 150 Hz range the locomotive works more or less as a *negative* resistance. That is, if a net harmonic is in this range the locomotive supplies energy to the net. Therefore the train is an active component to the net, perturbations are amplified. If a lot of passive components are removed it is possible, as the Swiss example showed, that the resonance is amplified and ends up in a brakedown.

One might ask if it really is efficient to use these complicated systems. Is it really worth it? Some of the reasons that the answer is 'yes' are stated here:

- Simple and robust engine
- Practically no maintenance of the system
- Electrical brake system (no mechanical parts)
- Small weight
- Negliable reactive power

A good reference for learning more about trains in general is [9] and to learn more about the network interaction issue of converter locomotives [8] and [3].

4 System Modeling in Time Domain

Here the motor side subsystems will be presented in more detail and when suitable also the mathematical models

4.1 Motor Side Voltage Converter

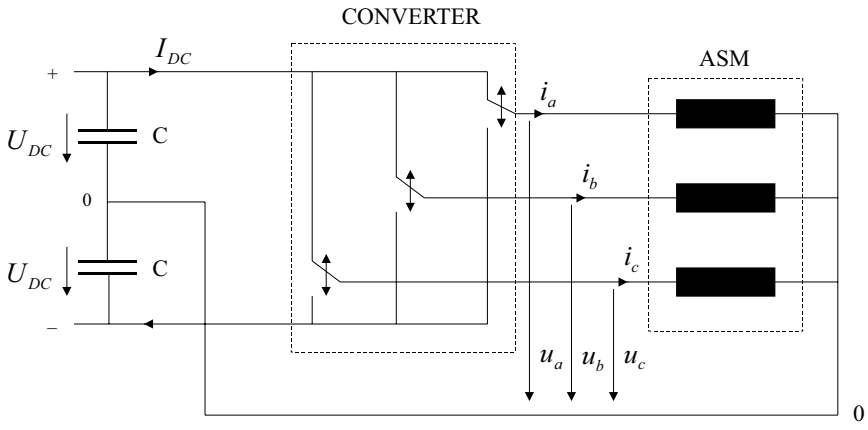

Figure 4: A simplified circuit describing the motor side of a converter locomotive.

In figure 4 the motor side of a converter locomotive is shown. As can be seen the converter is the connection between the DC-link and the engine. The converter is implemented with three switches, each one of them connected to one of the engine phases. Thus $u_{a,b,c}$ can take the values $\pm U_{DC}$. The switches are made of GTO-thyristors and contain no mechanical parts. Mechanical parts would be worn down quickly as the switching frequency is about 300 Hz. The state of each switch is given by $S_{a,b,c}$. $S_i = 1$ means $u_i = +U_{DC}$ and $S_i = -1$ means $u_i = -U_{DC}$.

As the three phase engine is a symmetric load it is enough to make the calculations with two coordinates. The three phases have a phase difference of 120° to one another. Therefore introduce the coordinate transformation $(a,b,c) \mapsto (\alpha,\beta)$. The new coordinates are stored in a complex number

$$\vec{x} = \frac{2}{3}\left(x_a e^{j0^\circ} + x_b e^{j120^\circ} + x_c e^{-j120^\circ}\right) = x_\alpha + j x_\beta$$

It is possible to invert this transformation by prescribing $x_\alpha = x_a$. You then get

$$\begin{aligned} x_a &= Re\{\vec{x}e^{j0^\circ}\} \\ x_b &= Re\{\vec{x}e^{-j120^\circ}\} \\ x_c &= Re\{\vec{x}e^{j120^\circ}\} \end{aligned}$$

The transformation is illustrated in figure 5. All motor calculations will be done in the $\alpha - \beta$ system. The results are then easy to transform back to the

three phase system. There are eight(2^3) different states of the swithches. Two of them result in a zero voltage vector, $S = (0,0,0)$ and $S = (1,1,1)$. The six other states result in vectors lying on a hexagon. These states are also shown in figure 5.

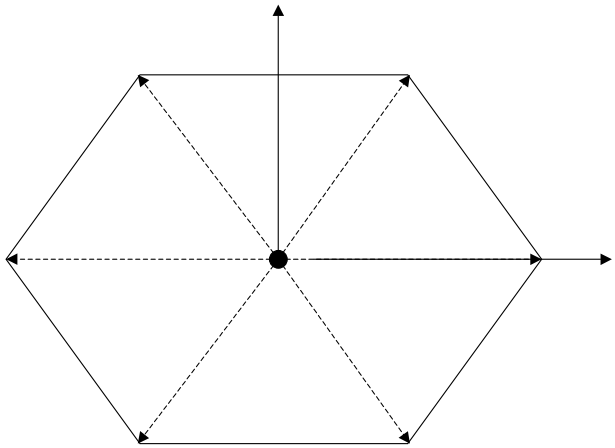

Figure 5: The coordinate transformation between (a,b,c) and (α,β). The eight different output states of the converter are also shown, six lying on a hexagon and two on the zero state.

Basically the task of the motor controller is to switch the voltage between these states so the motor flux vector moves on a circle. How to get the switching signals S differs in different controllers. Some controllers deliver S directly and just steer the flux on the hexagon. These methods are used at high speeds. For lower speeds you need voltage vectors lying between the states in figure 5. This can be obtained by making a time average of three states: the two closest to the wanted one on the hexagon and the zero state. Here Pulse Width Modulation (PWM) is used to obtain this average signal.

Another problem is to get a relation between the DC-link variables and the motor variables. It is possible to use the values of S. However it is easier to use a power balance. If the converter is idealized and the power loss is neglected the following relation holds:

$$p_{DC} = 2U_D I_{DC} = u_a i_a + u_b i_b + u_c i_c = \frac{3}{2}\left(u_\alpha i_\alpha + u_\beta i_\beta\right) = p_{motor} \qquad (12)$$

4.1.1 Pulse Width Modulation

The goal of Pulse Width Modulation is to approximate a signal $e_{s,sp}(t)$ by switching between two different voltages, $\pm U_{DC}$ in this case. Basically the method goes as follows: $e_{s,sp}$ is sampled with the period T_p. In the following period the voltage is switched once so that the average over T_p equals the input. To visualize how to calculate the switching times a triangle carrier wave often is used. An intesection of the carrier wave and the signal is followed by a switch. In figure 6 this is illustrated. How well the method works depends on the switching frequency, $f_{PWM} = 1/2T_p$. For high values of

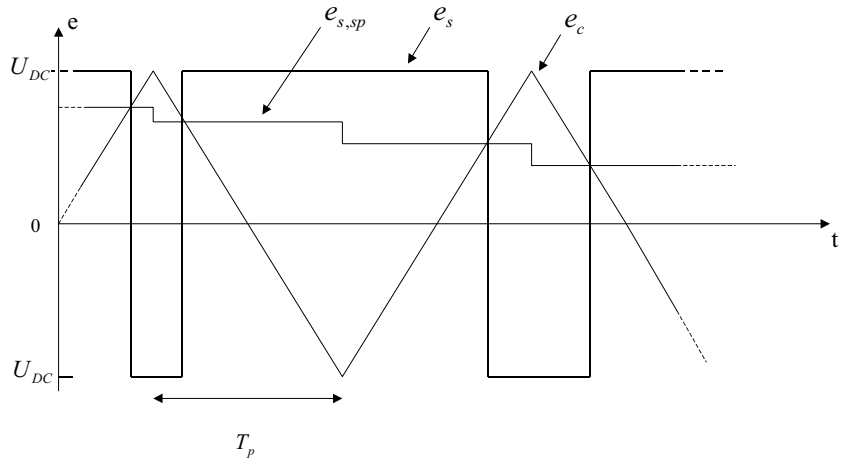

Figure 6: By the intersections of the carrier wave, e_c and the sampled signal $e_{s,sp}$ the output e_s is switched. If the sample period is small enough $e_{s,sp}$ is well approximated by e_s.

f_{PWM} the results are good. The output contains, of course, other frequencies than the wanted ones but these are located high up in the spectrum and can be filtered away. When the frequency of $e_{s,sp}$ is closer to f_{PWM} the method is less effective. The spectrum becomes more distorted and looks less like the one of $e_{s,sp}$. This is one of the reasons PWM only is used for low voltage frequency in the locomotive control.

4.2 Asynchronous Electrical Motor

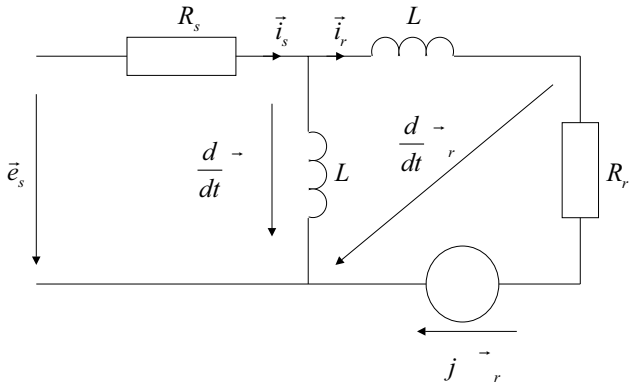

Figure 7: An equivalent circuit for the asynchronous electrical engine.

In figure 7 an equivalent circuit of a three phase ASM is shown in static coordinates. All the quantities are given in vector form according to the coordinate transformation given in the former section. To obtain the differ-

ential equations Kirchoffs laws are used in the stator and the rotor loops. By eliminating the the currents in the equations it is possible to express everything in the total flux $\vec{\Psi}_\mu$ and the rotor flux $\vec{\Psi}_r$. The exact procedure is given in [10]. The result is:

$$\frac{d}{dt}\vec{\Psi}_\mu = \vec{e}_s - R_s\left(\frac{1}{L_\mu}+\frac{1}{L_\sigma}\right)\vec{\Psi}_\mu + \frac{R_s}{L_\sigma}\vec{\Psi}_r \quad (13)$$

$$\frac{d}{dt}\vec{\Psi}_r = \left(j\omega - \frac{R_r}{L_\sigma}\right)\vec{\Psi}_r + \frac{R_r}{L_\sigma}\vec{\Psi}_\mu \quad (14)$$

$$M = \frac{3}{2L_\sigma}p\left(\Psi_{\mu\beta}\Psi_{r\alpha} - \Psi_{\mu\alpha}\Psi_{r\beta}\right) \quad (15)$$

$$\omega_s = \omega + \omega_r \quad (16)$$

Here M is the produced torque of the engine. It depends on p which is the number of magnetical pole pairs in the motor. There are three frequencies involved here: ω, ω_s and ω_r. ω is the mechanical angular frequency of the rotor. ω_s is electrical angular frequency, it differs from the mechanical frequency by the slip speed, ω_r. There is a relation between the delivered torque and the slip speed which is given in section 4.2.1.

Normally eq.(13)-(16) aren't used in this form in calculations. Instead they are normalized. The advantage is that all parameters then are given as ratios, so no absolute values are used. In this way different motor categories arise and the physical behaviour is easier to follow. The normalized quantities are given in table 1. The new equations become (17)-(21) simply by dividing the original ones with the respective normalized value.

$$T^*\frac{d}{dt}\vec{\psi}_\mu = n_0\vec{u}_s - \rho\vec{\psi}_\mu + \rho(1-\sigma)\vec{\psi}_r \quad (17)$$

$$T^*\frac{d}{dt}\vec{\psi}_r = (jn-1)\vec{\psi}_r + \vec{\psi}_\mu \quad (18)$$

$$m = 2(\psi_{\mu\beta}\psi_{r\alpha} - \psi_{\mu\alpha}\psi_{r\beta}) \quad (19)$$

$$n_s = n_r + n \quad (20)$$

$$\vec{y}_s = \frac{1}{1-\sigma}\vec{\psi}_\mu - \vec{\psi}_r \quad (21)$$

In table 1 E^* is the motor rated stator voltage amplitude. ω_0 is the corresponding angular electrical frequency. These values are chosen from thermal and magnetical considerations. In the following $E_0 = U_{DC,sp}$. Notice that ω_0 here is different from the theory section, here it is a motor parameter. It will not be used any more in the sequel. The new motor parameters are given in table 2

It is also possible to make a coordinate transformation of the motor equations to rotating coordinates by setting $\vec{x} = \vec{x}'e^{j\phi(t)}$ for every variable where $\dot{\phi}(t) = \omega_s(t)$. In these coordinates some relations are easier to obtain. In principle all calculations in the sequel are possible to do in rotating coordinates. The ISC-controller equations for instance are invariant under this coordinate transformation. In the sequel though the static coordinates will be kept as the results are easier to interpret.

To get a better feeling for ASM:s it is strongly recommended to to study [11] where a lot of qualitative and quantitative characteristics are shown.

Quantity	*Normalization Value*	*Normalized Quantity*
Voltage	$E^* = \frac{4}{\pi} E_0$	$u = \frac{e}{E^*}$
Flux	$\Psi^* = \frac{E^*}{\omega_0}$	$\psi = \frac{\Psi}{\Psi^*}$
Angular Frequency	$\omega^* = \frac{1}{T^*} = \frac{R_r}{L_\sigma}$	$n = \frac{\omega}{\omega^*}$
Current	$I^* = \frac{\Psi^*}{L_\sigma}$	$y = \frac{i}{I^*}$
Torque (per pole pair)	$M^* = \frac{3}{4} I^* \Psi^*$	$m = \frac{M}{M^*}$

Table 1: Normalized motor variables.

Rotor Time Constant	$T_r = \frac{L_\mu + L_\sigma}{R_r}$
Stator Time Constant	$T_s = \frac{L_\mu}{R_s}$
Time Constant Ratio	$\rho = \frac{T_r}{T_s}$
Motor Stray Time Constant	$T_\sigma = \frac{1}{\omega^*}$
Stray Ratio	$\sigma = \frac{L_\sigma}{L_\sigma + L_\mu}$
Frequency Ratio	$n_0 = \frac{\omega_0}{\omega^*}$

Table 2: Normalized motor paramters.

4.2.1 Stationary Harmonic Condition

When the mechanical frequency is constant and the stator voltage is purely sinusoidal it is possible to obtain a solution analytically. Then every electrical and magnetical quantity is varying sinusoidal with the frequency ω_s. The delivered torque is constant. To get these relations simply set $\vec{\psi}_\mu = \gamma e^{j\omega_s t}$ and insert in eq.(17)-(21). When n is constant the differential equations are linear and the other quantities must have a particular solution that is sinusoidal of the same frequency. Some results are

$$\vec{\psi}_\mu = \gamma e^{j\omega_s t} \tag{22}$$

$$\vec{\psi}_r = (\gamma \cos\vartheta) e^{j(\omega_s t - \vartheta)} \tag{23}$$

$$m = \gamma^2 \sin 2\vartheta \tag{24}$$

$$\tan\vartheta = n_r \tag{25}$$

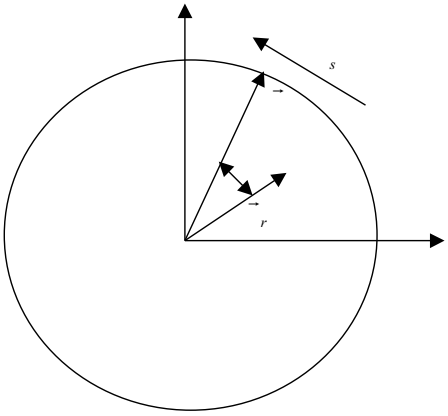

Figure 8: The fluxes under stationary harmonic conditions. The amplitude of the total flux is γ. The angle between the fluxes is related to the slip speed and the torque. When the angle is zero the torque also is zero.

$$n_r = \tan\left(\frac{1}{2}\arcsin\frac{m}{\gamma^2}\right) \tag{26}$$

$\vec{y}_s$ and $\vec{u}_s$ are easy to get by inserting the above relations into (17)-(21). The variables are visualized in figure 8. The torque equations show that when ϑ and the normalized slip speed n_r are small the relation to the torque almost is linear. This also implies that when the angle is negative the motor delivers a negative torque, that is, it works as a brake. In fact the engine then acts as a generator and it is possible to reverse the process and let the energy flow back to the railway net. Thus no mechanical parts are needed to stop the train.

4.2.2 Operating Areas and Control

When the control of the motor is considered some new parameters are used to part different control strategies and motor operating areas. The ratio between the first harmonic of the total flux and Ψ^* is called *field weakening ratio*, γ. The ratio between the first harmonic of the stator voltage and E^* is called a.

$$\gamma = \frac{\Psi_{\mu,0}}{\Psi^*}, \quad a = \frac{e_{s,0}}{E^*}$$

Two different operating areas then are defined:
Field Saturation Area: $\gamma = 1,\ 0 \leq a \leq 1,\ n_s \leq n_0$
Field Weakening Area: $\gamma < 1,\ a = 1,\ n_s > n_0$

The frequencies and the volatges are normally normaized once again in the controller equations:

$$k_n = \frac{n}{n_0}, \quad k_{ud} = \frac{U_{DC}}{U_{DC,sp}}$$

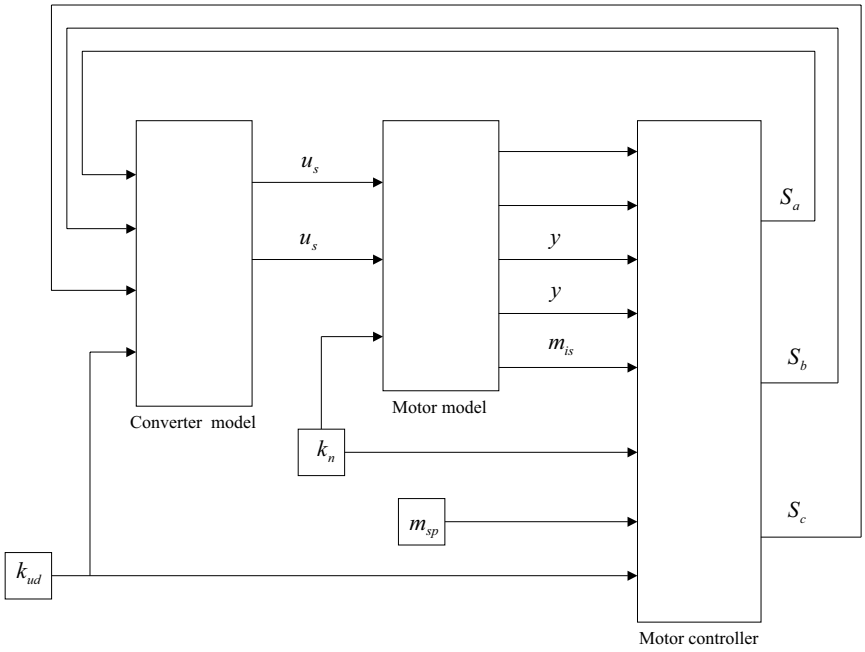

Figure 9: A flow diagram of the motor control system. k_{ud} is the DC-link voltage, k_n is the mechanical frequency and m_{sp} is the set point of the torque.

4.3 Motor Side Controllers

The locomotive has different control strategies in different speed ranges. There are three different structures: Indirect Self Control (ISC), Direct Self Control (DSC) and Field Weakening Direct Self Control (FW-DSC), of which the first will be treated in this report. The different strategies are used in different ranges of γ and a, see 4.2.2.

ISC is used when $\gamma = 1$ and $a < 0.3$ whereas DSC is used when $0.3 < a \leq 1$ and $\gamma = 1$. As the name discloses FW-DSC is used when $\gamma < 1$ and $a = 1$. All of them work with the total magnetic flux of the engine in one way or another. The direct self controllers are used when the train is moving with higher velocities. The converter then has to low switching frequency to be controlled by PWM. Instead the direct self controllers directly delivers the switching signals $S_{a,b,c}$.

Figure 9 shows the motor control system. As can be seen the flux components are directly fed to the controller. This is not the case in the real system. There the fluxes are reconstruced from measurable motor quantities such as currents with some kind of observer (Kalman or Luenberger for instance). In this report though the observer time constant is considered to be small in comparison to engine time constant, T_σ.

The main objectives of the motor controller is to follow the changes in the torque set point, magnetize the motor in a optimal way and maintain stability. It also has to take into account that the DC-link voltage not always is constant, for instance due to the pulsating power from the net . For this

reason there is a low-pass filter in the DC-link which should compensate for this, however some changes pass through and may influence the motor and the controller performance.

4.3.1 Indirect Self Control

The Indirect Self Control is used to control the engine under moderate speeds ($< 30\ km/h$). It calculates the necessary average motor voltage ($\vec{u}_s$)in order to steer the two control quantities: the torque and the flux, oriented through the total flux $\vec{\psi}_\mu$. ISC is a predictive control method and has both feed-forward and feed-back parts. The calculated voltages are fed to a voltage converter which uses PWM (Pulse Width Modulation) to apply the correct voltage to the ASM. The control of $\vec{\psi}_\mu$ is divided into two parts:

- to control the total flux so that $|\vec{\psi}_\mu| = \gamma$
- to control the angular velocity, ω_s of the total flux

The first objective means that the total flux is held on a circle of radius γ, which in this speed range should be 1. In that way the engine will work with optimal efficiency (magnetically saturated). The second objective controls the torque via the slip of the engine. According to the model equations for an ASM the torque is directly dependent on the slip (n_r). Furthermore this relationship is very close to linear in the ISC range.

$$k_\Psi = V_\Psi \left(1 - \frac{\psi_{\mu,is}}{\psi_{\mu,sp}}\right) \tag{27}$$

$$k_{nr,ff} = \frac{1}{n_0}\left(\frac{m_{sp}}{\gamma^2} + \frac{1}{8}\left(\frac{m_{sp}}{\gamma^2}\right)^3\right) \tag{28}$$

$$k_{nr,fb} = V_{md}\left(\frac{m_{sp} - m_{is}}{\gamma^2}\right) + \frac{T_i}{T_p}\int_{-\infty}^{t} \frac{m_{sp} - m_{is}}{\gamma^2} d\tau \tag{29}$$

$$k_{ns} = k_n + k_{nr,ff} + k_{n,fb} \tag{30}$$

$$u_{s,\alpha} = \frac{\rho(1-\sigma)}{n_0} y_\alpha + \frac{T_\sigma}{n_0 T_p} k_\Psi \psi_{\mu\alpha} - (1 + k_\Psi) k_{ns} \psi_{\mu\beta} \tag{31}$$

$$u_{s,\beta} = \frac{\rho(1-\sigma)}{n_0} y_\beta + \frac{T_\sigma}{n_0 T_p} k_\Psi \psi_{\mu\beta} + (1 + k_\Psi) k_{ns} \psi_{\mu\alpha} \tag{32}$$

To calculate the correct momentaneous voltage, $\vec{u}_s$, it is divided into one radial and one angular part. Each is controlled independently and steers the flux in the corresponding direction, see figure 10. The radial voltage component is controlled through k_Ψ which is the output of a simple P-controller. The angular voltage has a feed-forward part based on the steady-state sinusoidal torque-slip relation (26). A Taylor approximation (28) is implemented to reduce computation time, which in real time is critical. To compensate for this approximation and other errors a PI-controller is connected in parallell (29). The two voltage components are then projected back to the $\alpha - \beta$ coordinate system, which gives (31) and (32).

In the above equations V_Ψ, V_{md} and T_i are controller parameters. T_p is the time period in which the voltage is averaged and the switching period of

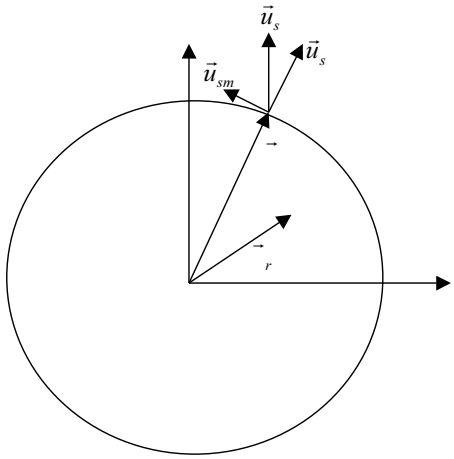

Figure 10: The total flux, $\vec{\psi}_\mu$ is controlled on a circle of radius γ by the voltage $\vec{u}_s$.

the voltage converter. k_n is the normalized mechanical angular frequency. For a more detailed description of the IFC with all the steps more carefully motivated see [10].

4.4 Mechanics

The mechanics of a locomotive and a train is very complicated if all effects are to be modeled. The forces and the torques are very large and the contact forces to the railway must be taken into account. The main task of this work is not to make models of the mechanics so a very simplified linear model based on the torque equation

$$\sum_i M_i = K\dot{\omega}$$

is used. M_i are the torques and K is the moment of inertia which represents the mass of the train. ω is the mechanical angular frequency of the motor. A friction torque, M_F, is introduced that is proportional to the angular frequency. The model in normalized quantities then becomes:

$$m_{is} + m_F = m_{is} - Ln = K_{train}\dot{n}$$

$$\Leftrightarrow$$

$$\dot{n} + \frac{L}{K_{train}}\, n = \frac{1}{K_{train}}\, m_{is} \tag{33}$$

L is a friction coefficient. The time constant of the system is L/K_{train}. When the applied torque is constant the mechanical frequency will stabilize around

$$n = \frac{m_{is}}{L}$$

5 System Modeling in Frequency Domain

In this section the subsystems from section 4 will be modeled in frequency domain. The methods used were presented in the theory section so here only the different approximations are shown. Some examples will be made to see how good the different subsystems are modeled. The models are compared to results from `Simulink`-implementations of the equations.

The overall system will not be closed until the next chapter where the question of finding a linearization(operating) point also will be answered.

5.1 Motor Side Voltage Converter

The converter could be seen as a switch that connects its output to different input lines, in our case $\pm U_{DC}$. The time domain expression of this for one phase is:

$$e_s(t) = S(t)U_{DC}(t)$$

where $S(t)$ is the switching signal (± 1) and $U_{DC}(t)$ the time dependent DC-link voltage level. The relation is a convolution in frequency domain. This could be modeled according to 2.4.1. The problem is to get $S(t)$. In the ISC-range PWM is used to get this switching signal, $S(t) = G\{e_{s,sp}(t)\}$. In order to make it simple in the following the converter and the PWM will be modeled together. This is done in the next section.

In section 4.1 a power balance, eq.(12) was used to get a relation between the DC-link and motor variables. The balance must be rewritten in frequency domain. Once again it is a convolution and section 2.4.1 can be used. The relation becomes:

$$2\mathcal{U}_{DC}\Delta I_{DC} + 2I_{DC}\Delta\mathcal{U}_{DC} = \frac{3}{2}\left(\mathcal{U}_\alpha\Delta I_\alpha + I_\alpha\Delta\mathcal{U}_\alpha + \mathcal{U}_\beta\Delta I_\beta + I_\beta\Delta\mathcal{U}_\beta\right) \quad (34)$$

$\Delta(\cdot)$ indicates the spectrum difference to the operating point. In the following the right hand side is going to be calculated in dependence of changes of the set points of the controller. If the DC-link spectrums are known at the operating point of the motor, it is possible to get a relation between $\Delta\mathcal{U}_{DC}$ and ΔI_{DC} by simple matrix algebra. Then we have the desired admittance matrix of the motor side.

5.1.1 Pulse Width Modulation

How PWM works was described in 4.1.1. There it wasn't mentioned that before the switching point is calculated the voltage in the DC-link is measured. By doing that possible changes in the DC-link voltage level are partially compensated for. In the sequel the assumption is made that the DC-link doesn't influence the relation between the input to the PWM , $e_{s,sp}$, and the output from the converter, e_s.

We will now try to get a HTM between the two spectrums $\mathcal{E}_{s,sp}$ and $\mathcal{E}_s$. As the relation is nonlinear we use the methods in section 2.4. Therefore we try to evaluate a Jacobian (HTM) at a operating point $\mathcal{E}_{s,sp}$. A HTM for this case is derived in A. The result there gives a HTM $\mathcal{G}_{PWM}$ and the relation:

$$\delta\mathcal{E}_s = \mathcal{G}_{PWM}\,\delta\mathcal{E}_{s,sp} \quad (35)$$

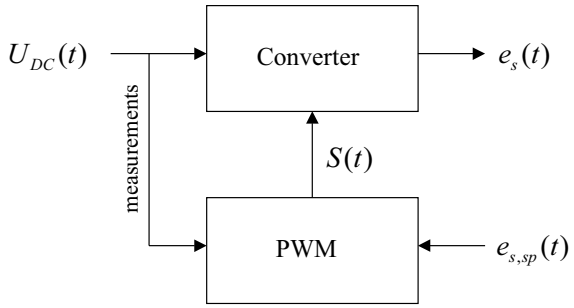

Figure 11: Illustration of the signal flow in the converter unit.

where $\delta(\cdot)$ indicates the difference to the operating point spectrums. A converter with an infinite switching frequency would result in a matrix $\mathcal{G}_{PWM}$ that equals an identity matrix. But here we have a finite frequency at about 300 Hz, which results in time delays and sidebands in the output. How well the input signal is imitated and how well the model works will be shown in an example.

Example: Sidebands from PWM

The operating point in this example is

$$e_{s,sp}(t) = 0.4\cos\omega_0 t, \;\; \omega_0 = 2\pi/0.06, \;\; T_p = 0.002, \;\; N = 15, \;\; Q = 20$$

(See A for more details. The real real representation of the Fourier series is used in this example.) Then a perturbation in the third harmonic is introduced as

$$\delta e_{s,sp}(t) = \delta a_3 \cos 3\omega_0 t + \delta b_3 \sin 3\omega_0 t$$

The question is now what the perturbations in the spectrum of $e_s(t)$, δA_k and δB_k $k \in Z$, are. Ideally there would only be changes for $k = 3$. But as there are sidebands we will see changes for $k \neq 3$. The results are plotted in frequency domain in figure 12.

As can be seen there is almost a perfect fit between the model and the time simulations. The third coefficient shows that the amplitude of the output is almost equal to the amplitude of the input, as it should. But there is a time lag introduced as the outputs are not exactly a sine or a cosine. If that was the case the points would lie on the coordinate axes. Also the other frequencies produced are well described by the model.

The problem is frequencies for other k arise. For some k such as 3,11,13,17, 19,... the dependance on the input is linear to a large extent as can be seen in figure 12. For other k such as $7, 9, 15, 21, \ldots$ the dependance lacks a linear part and is thus not describable with the HTM. When the perturbation is larger than 0.1 these coefficients starts to have the same order of magnitude as the one with linear dependance and the use of the model starts to be questionable. The error analysis in A.1 turns out to be far to pessimistic. The largest error is in harmonic 15. The analysis gives an upper bound that is about 1000 times larger than the real error.

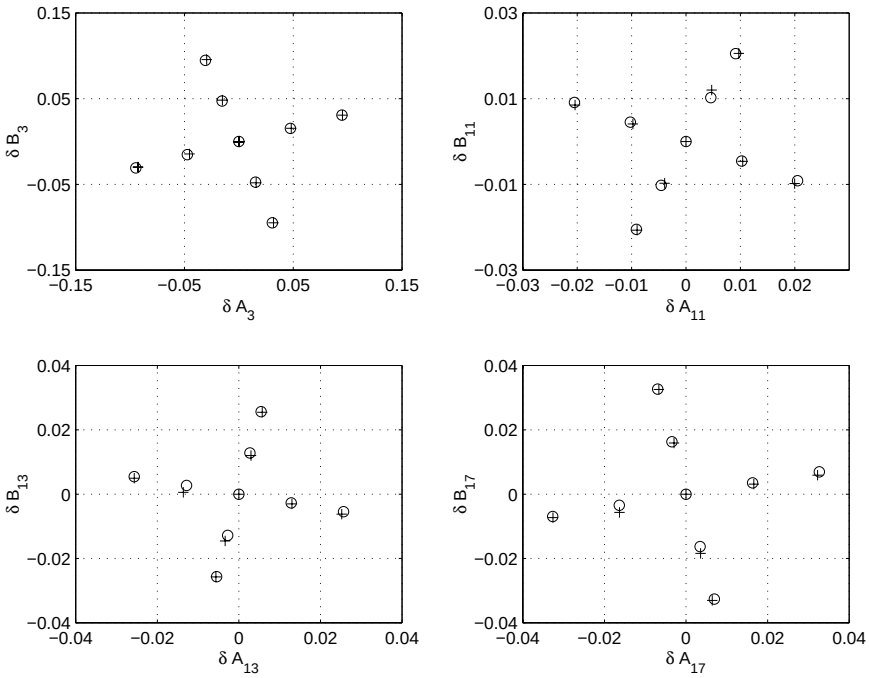

Figure 12: The deviations in the output spectrum $\mathcal{E}_s$ are plotted for $k = 3, 11, 13, 17$. There are two test series: $\delta a_3 = -0.1, -0.05, 0, 0.05, 0.1$; $\delta b_3 = 0$ and vice versa. (o) comes from the HTM and (+) comes from time simulations in Simulink. Discrete Fourier Transform was used to get the coefficients from the simulations.

Example: LTI part of PWM

Here the same operating point as in the former example is used. The absolute values of the HTM is plotted in figure 13. The diagonal is the LTI part of the function. It is plotted in Bode form in figure 14 where a couple of time simulated values also are included.

The absolute values of the HTM show that the distances between the sidebands are 250 Hz. Many times it is not interesting to study the high frequencies that the sidebands give rise to. The ASM is very inductive and these high voltage frequencies don't produce large stator currents. Thus the energy in these frequencies is of minor importance. It is often sufficient to use the diagonal part of $\mathcal{G}_{PWM}$.

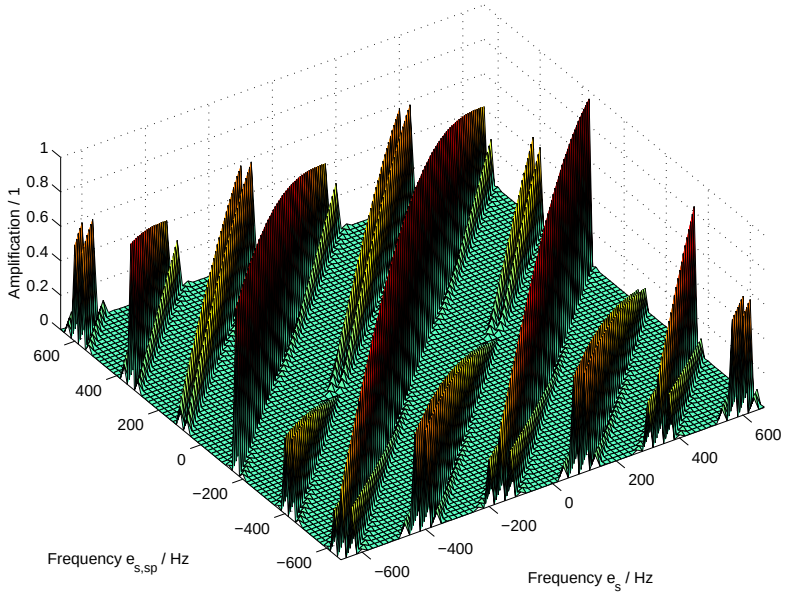

Figure 13: The absolute values of $\mathcal{G}_{PWM}$ is plotted. As can be seen a lot of sidebands are created, all of them with high frequency shift. Notice the converter has a switching frequency of 250 Hz.

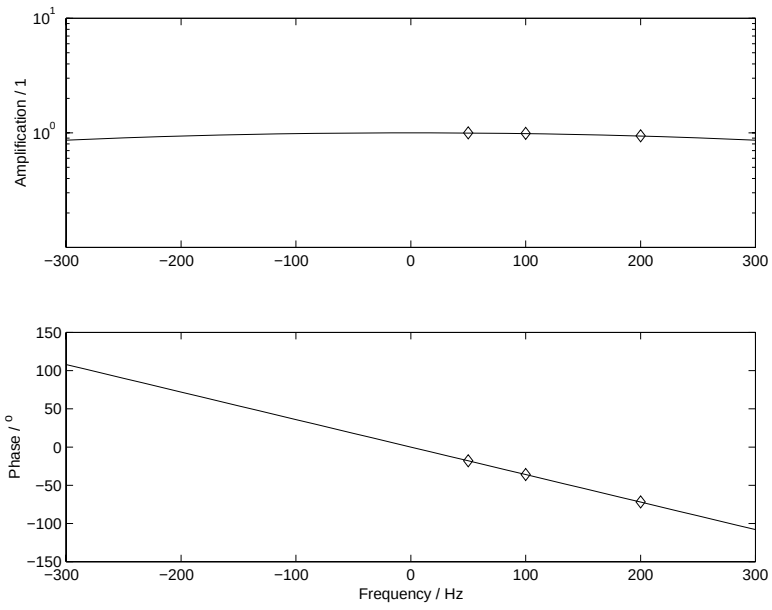

Figure 14: The LTI (Bode) part of $\mathcal{G}_{PWM}$ in figure 13 is plotted. The solid line comes from the model and ($\Diamond$) comes from time simulations ($\delta a_3 = 0.1$). The measurements fit fine with the model.

5.2 Asynchronous Electrical Motor

The ASM equations in 4.2 are here going to be studied in frequency domain. The treatment is highly dependent on the mechanical frequency n. If n is constant during the modeling the motor equations become purely linear and the frequency domain analysis reduces to the classical one, as long as the torque equation is left out. The torque equation (19) is nonlinear in any case, but if the goal is to create an admittance matrix of the motor this can be left out. Unfortunately we need the torque in the analysis later on.

If the motor frequency is changing we have a time dependent multiplication of the rotor flux and the mechanical frequency. Normally n is coupled to the torque, m, via the mechanics. That means if m_{sp} changes these changes will propagate through the system and end up as changes in n, thereby making the system equations nonlinear. In the following section a possibilitiy will be presented where these nonlinearities have been approximated in order to to make a frequency domain model.

5.2.1 Mechanical Frequency Prescribed

The ASM equations in static coordinates are given in eq.(17)-(18). A first step in frequency analysis of these relations would be to prescribe the value of n. If n is constant we have a LTI system. By letting n be a periodic function that is not influenced by any other variables we have a Linear Time Periodic system. Then the exact HTM (admittance matrix in this case as only current and voltage are under consideration) can be constructed given that the number of frequencies used, N, is large enough. The matrices in eq.(2)-(3) then are

$$A(t) = \frac{1}{T^*}\begin{pmatrix} -\rho & 0 & \rho(1-\sigma) & 0 \\ 0 & -\rho & 0 & \rho(1-\sigma) \\ 1 & 0 & -1 & -n(t) \\ 0 & 1 & n(t) & -1 \end{pmatrix}$$

$$B(t) = \frac{1}{T^*}\begin{pmatrix} n_0 & 0 \\ 0 & n_0 \\ 0 & 0 \\ 0 & 0 \end{pmatrix}$$

$$C(t) = \begin{pmatrix} 1/(1-\sigma) & 0 & -1 & 0 \\ 0 & 1/(1-\sigma) & 0 & -1 \end{pmatrix}$$

$$v(t) = (u_\alpha \;\; u_\beta)^T \quad i(t) = (y_\alpha \;\; y_\beta)^T \quad x(t) = (\psi_{\mu\alpha} \;\; \psi_{\mu\beta} \;\; \psi_{r\alpha} \;\; \psi_{r\beta})^T$$

The admittance matrix $\mathcal{Y}(\lambda)$ is calculated accordning to eq.(7).

Example: Mechanical Frequency Prescribed and Time Periodic

To see how many frequencies are needed in the admittance matrix and how fast the current converges a test is made. The motor voltages are purely sinusoidal, $u_\alpha = \cos\omega t$ and $u_\beta = \sin\omega t$ ($\lambda = 0$). Then the mechanical frequency is driven as $k_n = 1 + 0.2\cos\omega_0 t$. Here are $\omega = 5\omega_0 = 20\pi$ ($T = 0.5$). The current component y_α is plotted in time domain over one period T

in figure 15. The results of the matrix calculations are plotted for different values of N. As it can be seen it has almost converged after only 8 frequency components.

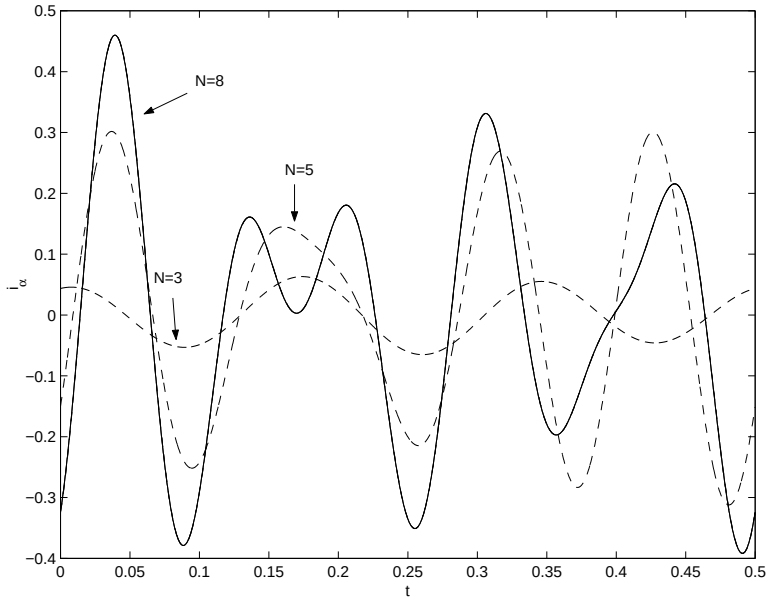

Figure 15: The α-current component is plotted when the engine is driven by purely sinusoidal voltage but has a periodically changing motor frequency. The matrix approximation results are also plotted for different N. The solid line comes from time simulation and is almost identical with the HTM result when N=8. Notice the hard non-LTI behavior between voltage and current, if k_n was to be constant the current would be a single sinusoidal of frequency ω.

5.2.2 Mechanical Frequency as Input

The problem is that the mechanical frequency later is going to be coupled to the torque. In order to comply with these terms an approximation of the product is made according to 2.4.1. In that way the mechanical frquency can be treated as an input. At the same time an analog approximation of the torque is implemented. After these changes the ASM can be approximated as a LTP system. The changes in the matrices look like:

$$B(t) = \frac{1}{T^*} \begin{pmatrix} n_0 & 0 & 0 \\ 0 & n_0 & 0 \\ 0 & 0 & -\psi_{r\beta}(t) \\ 0 & 0 & \psi_{r\alpha}(t) \end{pmatrix}$$

$$C(t) = \begin{pmatrix} 1/(1-\sigma) & 0 & -1 & 0 \\ 0 & 1/(1-\sigma) & 0 & -1 \\ -2\psi_{r\beta}(t) & 2\psi_{r\alpha}(t) & 2\psi_{\mu\beta}(t) & -2\psi_{\mu\alpha}(t) \end{pmatrix}$$

$$v(t) = (\Delta u_\alpha \;\; \Delta u_\beta \;\; \Delta n)^T \quad i(t) = (\Delta y_\alpha \;\; \Delta y_\beta \;\; \Delta m)^T$$

Now the equations are formulated in deviations from a stationary solution $\vec{\psi}_\mu$ and $\vec{\psi}_r$. That means an operating trajectory of the engine has to be known and the predicted results from these equations are related to this. To find an operating trajectory time simulations could be used, but that is not so attractive. In 4.2.1 a solution is given where m_{is} and n are constant. This solution could be chosen to linearize around. In the example below this is done.

Example: Mechanical Frequency as Input

As in the former example the motor is driven by purely sinusoidal voltage. Now perturbations in k_n is introduced by adding a harmonic, that is $k_n = 1 + A\cos\omega_0 t$ where A is the size of the perturbation. The torque and the current of the engine is then studied. Notice the difference from the former example: here two approximations are included, of the mechanical frequency and of the torque. In figure 16 and 17 the time domain appearance of the current and the torque are displayed over one period for two particular cases.

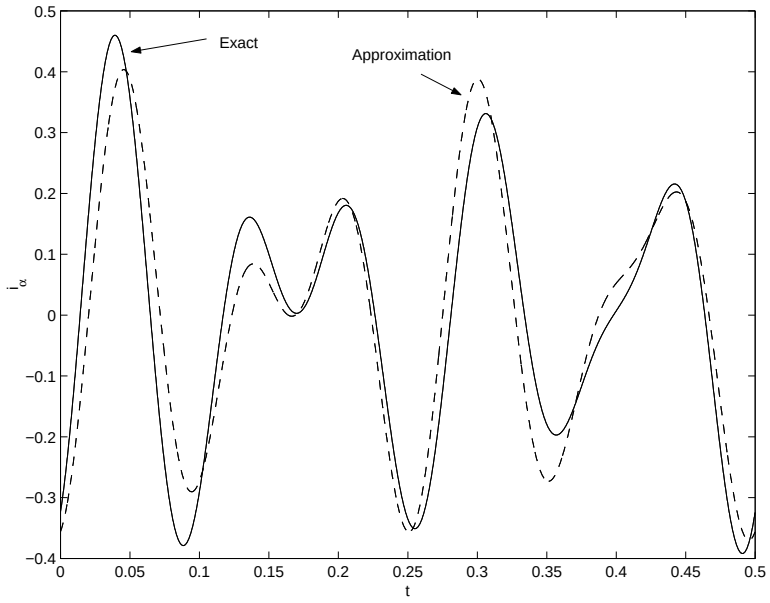

Figure 16: The absolute $(y_\alpha + \Delta y_\alpha)$ α-current component is plotted when k_n is perturbed with $0.2\cos\omega_0 t$. The approximation is plotted when $N = 8$, larger values of N don't bring anything more. The energy error is 5.8%. The energy of a signal $x(t)$ is defined as $\int_t^{t+T} x(\tau)^2 d\tau$.

As can be seen the current is better approximated, which sounds reasonable because then only the approximation of the mechanical frequency is needed. In fact the approximated torque reduces to one single harmonic of frequency ω_0 because all the other terms of m_{is} cancels. It clearly looks like

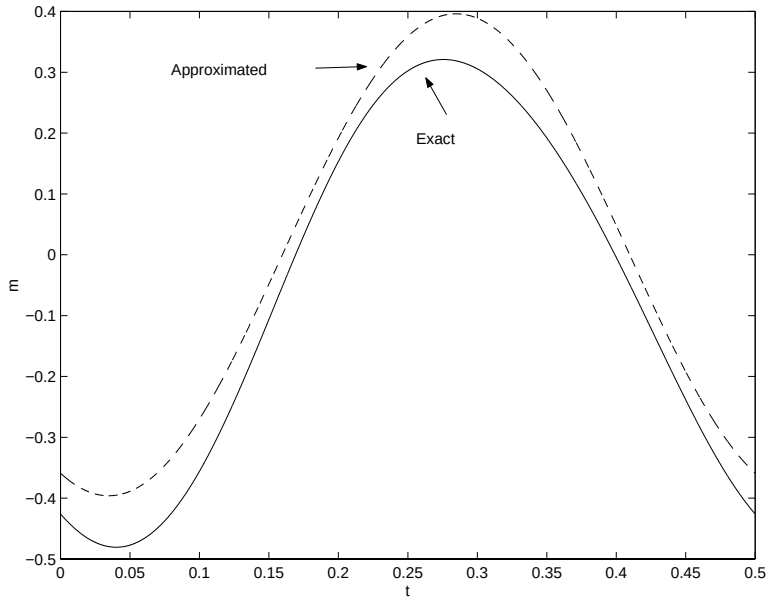

Figure 17: The total torque is plotted when $k_n = 1 + 0.1\cos\omega_0 t$. The approximation is plotted when $N = 8$, larger values of N don't bring anything more. The energy error is 7.6%.

the torque is going to set the border between useful and not useful of this model. Notice that it doesn't bring anything to use more frequencies than 8. The reason for this is that the current can be almost exactly described with 8 components, see the former example. So the errors here are due to the to the approximations of the nonlinearities.

In spite of the large perturbations the approximations capture the main behavour of the engine. When studying the current a perturbation of 20% in the frequency is no problem. When the torque is studied a perturbation of 10% is acceptable. The model shown in this example will be used in the analysis section later and be connected to the controller. The output and input vectors are going to be changed as the controller and the mechanics need more states to be modeled.

5.3 Motor Side Controllers

The goal is to model the controller so that a harmonic transfer matrix can be constructed. If the controller is given by explicit relations (ISC for example) this could be done according to the method in 2.4.1. If it's highly nonlinear (DFC for example) more unconventional methods must be used.

There are two input vectors to the controller: $y(t)$ and $u_{ref}(t)$. $y(t)$ is the output of the engine and $u_{ref}(t)$ is the set point of the controller. In the frequency domain the relationship can be formulated with HTM:s as:

$$\mathcal{U} = \mathcal{E}\mathcal{Y} + \mathcal{F}\mathcal{U}_{ref} \tag{36}$$

The problem is to get $\mathcal{E}$ and $\mathcal{F}$. In the following these matrices will be given for the ISC-controller.

5.3.1 Indirect Self Control

To obtain harmonic transfer matrices for the ISC approximations of the equations (27)-(32) are made. As was the case when the induction engine was approximated in 5.2.2 we assume a periodically time varying trajectory is known. As was told in the ASM example such a solution can be determined a-priori when m_{sp}, k_n and k_{ud} are constant. Otherwise a solution can be obtained via time domain simulations, for example with `Simulink` models. All quantities in this paragraph that are time varying have the same fundamental time period, T.

The approximations of (27) to (32) are made in a couple of steps. First of all the approximation $k_\Psi = 0$ is made. Simulations have shown that this variable is very small and can be neglected. It also is comfortable because then the absolute value of the flux, ψ_{is} doesn't have to be calculated. That variable may be hard to calculate in static coordinates. The nonlinearities are the multiplications of the flux components and the normalized electrical frequency, k_{ns}. These are approximated through 2.4.1. Here the integral term of the torque is left out for simplicity. It will be included in the analysis in the next section by adding an extra state in the engine model. The controller may now be written in matrix form:

$$\Delta u(t) = E(t)\Delta y(t) + F(t)\Delta u_{ref}(t)$$

where

$$\begin{aligned} \Delta u(t) &= (\Delta u_\alpha \;\; \Delta u_\beta \;\; \Delta n)^T \\ \Delta y(t) &= (\Delta \psi_{\mu\alpha} \;\; \Delta \psi_{\mu\beta} \;\; \Delta y_\alpha \;\; \Delta y_\beta \;\; \Delta m_{is})^T \\ \Delta u_{ref}(t) &= (\Delta m_{sp} \;\; \Delta n)^T \end{aligned}$$

$$E(t) = \begin{pmatrix} 0 & -k_{ns}(t) & \frac{\rho(1-\sigma)}{n_0} & 0 & \psi_{\mu\beta}(t)V_m/\gamma^2 \\ k_{ns}(t) & 0 & 0 & \frac{\rho(1-\sigma)}{n_0} & -\psi_{\mu\alpha}(t)V_m/\gamma^2 \\ 0 & 0 & 0 & 0 & 0 \end{pmatrix}$$

$$F(t) = \begin{pmatrix} -\psi_{\mu\beta}(t)(V_m + \frac{1}{2n_0})/\gamma^2 & -\psi_{\mu\beta}(t)/n_0 \\ \psi_{\mu\alpha}(t)(V_m + \frac{1}{2n_0})/\gamma^2 & \psi_{\mu\alpha}(t)/n_0 \\ 0 & 1 \end{pmatrix}$$

The HTM:s of these are just Toeplitz matrices with the Fourier components of $E(t)$ and $F(t)$ as components. As the approximations meant neglecting quadratic terms the error is of this order. How well these approximations work will be shown in the closed loop analysis.

5.4 Mechanics

The mechanics was modeled with a simple linear time invariant differential equation, (33). Thus the results from section 2.2 can be applied straight

forward. The transfer function of the system is

$$\frac{N(s)}{M_{is}(s)} = G_{mech}(s) = \frac{1}{K_{train}s + L} \tag{37}$$

and results in a diagonal HTM.

Thus the mechanics is a simple first order damper without a resonance frequency. Later on a more complex model which includes the known mechanical resonance frequencies would be interesting to include in the closed loop system.

6 Analysis

In this section the frequency domain models of the subsystems will be connected to form a closed loop system. An operating point will be chosen and motivated. Then some tests of the system are going to be performed. The aim of these tests are to see how a harmonic change in a quantity such as U_{DC} or m_{sp} effect the other quantities, that is to construct a generalized transfer function (HTM). The questions to be answered are:

- What output frequencies are created?
- What is the amplitude and phase of the output? Risk for resonance?
- How do the model parameters influence the output?

The method to study the system is to calculate different HTM:s. The structure of the matrix holds a lot of information of the system. A strict diagonal matrix is equivalent to a LTI system and by plotting the diagonal a classical Bode plot is obtained. When the output contains sidebands the matrix becomes banded. These bands could also be plotted in Bode-style but with the important difference that the sideband frequency isn't the same as the input frequency, there is a constant difference. The amplitude of the output frequencies can be used to locate resonance conditions. Perhaps it is possible to influence the resonance peaks in some way.

To see how good the approximations are and how large perturbations they can handle the results are compared to time domain simulations. The time domain simulations are made in `Simulink` and consist of implementations of the equations and systems in section 4. A fifth order Dormand-Prince differential equation solver is used in the simulations. To compare the results the time or the frequency domain appearance is plotted from the model and the time simulation. The time domain results are plotted over one fundamental period. The frequency domain results are obtaind with Discrete Fourier Transform (DTF) of the time simulations. The amplitude and phase is then plotted in Bode diagrams.

How good can the results be? Quite a lot of approximations are done and already in 5.2.2 the error of the torque was fairly large. On the other hand the perturbations there were large, they could be said to be of maximal tolerable size. In real situations they normally would not occur. Thus there might be errors in the size of the predicted results but the overall behaviour of the interaction should be well described.

6.1 Closed Loop System

In order to analyze the system we have to combine all the subsystems modeled in section 5, that is to close the controller-engine-mechanics loop. Then the influence on and from the DC-link has to be modeled. One way of doing this is to make a HTM of each subsystem and then combine them to get the final matrix. If the symbols in figure 18 are used the results are:

$$\begin{aligned} \mathcal{Y} &= \overbrace{(I - \mathcal{G}_{ASM}\mathcal{G}_{mech})^{-1}\mathcal{G}_{ASM}}^{\mathcal{G}_{sys}}\mathcal{U}_1 \\ \mathcal{U}_1 &= \mathcal{G}_{PWM}(\mathcal{E}\mathcal{Y} + \mathcal{F}\mathcal{U}_{ref}) \end{aligned}$$

and the HTM of the system is

$$\hat{\mathcal{G}} = \left(I - \mathcal{G}_{sys}\mathcal{G}_{PWM}\mathcal{E}\right)^{-1}\mathcal{G}_{sys}\mathcal{G}_{PWM}\mathcal{F} \tag{38}$$

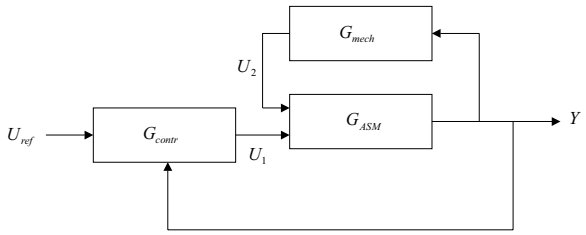

Figure 18: A schematic picture of the closed loop with the engine, the mechanics and the controller.

The problem here is when creating HTM:s of dynamical systems, as the engine and the mechanics, or when closing loops, you need to solve a linear equation system each time. As some of these matrices tend to be quite badly conditioned you should avoid to solve many systems to avoid unnecessary numerical inaccuracy. To solve many large scale linear systems also is time consuming. The advantage is that the model becomes very modular with one matrix for each component.

Instead it is possible to combine the matrices and to solve *one* linear equation system. For example the mechanics can be modeled together with the engine in the $A(t)$ matrix. With the components described in section 5 we have to introduce two more states to close the loop. First of all the integral part of the controller needs a state, $M_I = \int_{-\infty}^{t} m_{sp} - m_{is} d\tau$, which is added to the state vector x. This variable is then used as input to the controller, so $E(t)$ has to be slightly modified as well as $A(t)$. In order to model the mechanics the state Δn is moved from the reference input vector u_{ref} to x. The dynamics of the vehicle is then included in $A(t)$. The vectors of the model include the following states:

$$\begin{aligned} x &= \left(\Delta\psi_{\mu\alpha}\ \Delta\psi_{\mu\beta}\ \Delta\psi_{r\alpha}\ \Delta\psi_{r\beta}\ M_I\ \Delta n\right)^T \\ U_{ref} &= \Delta m_{sp} \\ y &= \left(\Delta\psi_{\mu\alpha}\ \Delta\psi_{\mu\beta}\ \Delta y_{\alpha}\ \Delta y_{\beta}\ \Delta m_{is}\ M_I\ \Delta n\right)^T \end{aligned}$$

The system of equations then becomes: $(\lambda = 0)$

$$\begin{aligned} \mathcal{N}\mathcal{X} &= \mathcal{A}\mathcal{X} + \mathcal{B}\mathcal{U}_1 \\ \mathcal{Y} &= \mathcal{C}\mathcal{X} \\ \mathcal{U}_1 &= \mathcal{G}_{PWM}\left(\mathcal{E}\mathcal{Y} + \mathcal{F}\mathcal{U}_{ref}\right) \\ \mathcal{N} &= \text{blkdiag}\{jk\omega_0 I\},\ \ \forall k \in Z \end{aligned}$$

The harmonical transfer matrix $\hat{\mathcal{G}}$ of the system is

$$\hat{\mathcal{G}} = \left(\mathcal{N} - \mathcal{A} - \mathcal{B}\mathcal{G}_{PWM}\mathcal{E}\mathcal{C}\right)^{-1}\mathcal{B}\mathcal{G}_{PWM}\mathcal{F} \tag{39}$$

Note that $\mathcal{G}_{PWM}$ not exactly is the HTM presented in section 5.1.1. As not only the voltages are fed to the engine model, but also for example the mechanical frequency, it has to be extendend with identity matrices. The other variables are not influenced by the PWM. $\mathcal{G}_{PWM}$ also has to be transformed so it can be used with the complex Fourier series.

Until now the DC-link hasn't been considered. As was told in section 5.1 the interaction between the motor and the link is modeled with a power balance in frequency domain. When choosing an operating point of the motor side the DC-link voltage and current spectrums are known. They are then transformed to HTM:s: $\mathcal{U}_{DC}$ and I_{DC}. The change of the needed power of the engine depends on $\mathcal{U}_{ref}$. $\hat{\mathcal{G}}$ gives the change in the stator currents, and the stator voltages are given by the controller relations. The current and the voltage spectrums are convoluted to get the power spectrum, eq.(34). The engine side power HTM is called $\mathcal{G}_p$. The power balance then becomes:

$$I_{DC}\Delta\mathcal{U}_{DC} + \mathcal{U}_{DC}\Delta I_{DC} = \frac{1}{2}\mathcal{G}_p\mathcal{U}_{ref}$$

$$\Leftrightarrow$$

$$\Delta I_{DC} = \mathcal{U}_{DC}^{-1}\left[\frac{1}{2}\mathcal{G}_p\mathcal{U}_{ref} - I_{DC}\Delta\mathcal{U}_{DC}\right] \tag{40}$$

Notice that when $\mathcal{U}_{ref} = 0$ the engine side works as a negative resistor which might inflict stability problems in the DC-link. Therefore in the real system $\mathcal{U}_{ref}$ is coupled to $\Delta\mathcal{U}_{DC}$. So when the DC-link voltage increases the set point of the torque automatically increases to absorb the extra power and thereby stabilizing the link. In time domain this relation looks like

$$m_{sp,new} = \left(\frac{U_{DC,is}}{U_{DC,sp}}\right)^2 m_{sp} \tag{41}$$

6.2 Operating Point

In order to work with the models a stationary solution has to be known. In section 4.2.1 a solution of the the motor equations was presented. It would be nice to use it because then all calculations can be done without first making any simulation or any iterative procedure. This solution meant that the main flux followed a circle with a constant frequency, ω_s. The question is, how well does the flux follow a circle under real conditions with voltage converters? If some tests are made it is clear that as long as the electrical frequency is small compared to the converter switching frequency the circle is well reproduced, see figure 19. If the spectrum of the total flux is studied the first not wanted harmonic comes at $2\pi/T_p$. Normally such high frequencies are not under consideration.

To get the DC-link operating point the power balance is used. Under the assumption above the engine needs constant power. A solution is easily found when the DC-link voltage is constant, the current is then also constant. The problem comes when the DC-link voltage is time periodic. Then the question is to find another time periodic function which multiplied with the first gives a constant. To find a solution a convolution matrix is made of the

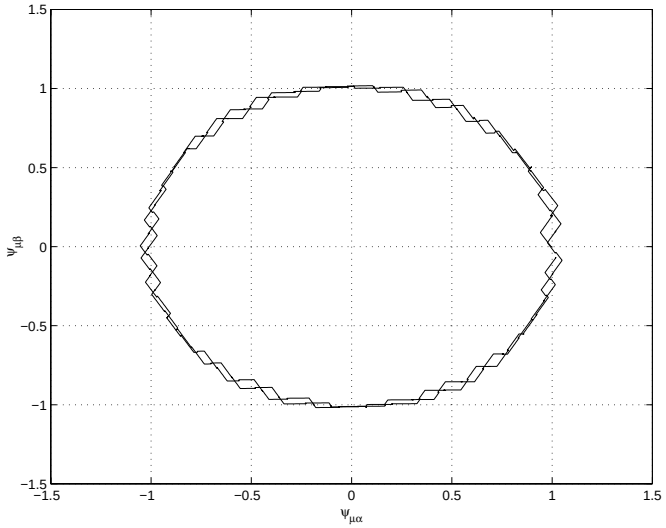

Figure 19: Two periods of the total flux are plotted from Simulink simulations. $k_n = 0.2$, $m_{sp} = 0.2$ and $T_p = 0.002\ s$.

DC-link voltage spectra. To get a quadratic matrix it is truncated and you get a Toeplitz matrix just like the ones in section 2.4.1. To get the current spectra the linear equation system

$$[\text{Toepliz, } \mathcal{U}_{DC}] \times [\text{unknown spectra, } I_{DC}] = [\text{power spectra}] \qquad (42)$$

has to be solved.

When a DC-link voltage compensator like eq.(41) is added, the engine no longer draws a constant power when the voltage varies. A way to find an operating point could be as follows:

1. Choose an operating point DC-link voltage spectra, U_{DC}.
2. Choose a constant value of m_{sp} (and n if no mechanics is included).
3. Calculate the spectrum $m_{sp,new}$ and use the constant part to calculate $\hat{\mathcal{G}}$.
4. Calculate the total power of the motor from $\hat{\mathcal{G}}$.
5. Insert U_{DC} and the power in eq.(42) and solve it for the operating point DC-link current.
6. Goto 1. if the DC-voltage spectrum changes and use the obtained motor fluxes as the new motor linearization point.

The method will be illustrated in section 6.5.

6.3 Test of Closed Loop without Mechanics

Here a test of the closed loop system will be performed. In this test the mechanics is not included so there are no connection between the mechanical frequency and the torque. The mechanics will be included in the next example. By studying the torque and the mechanical frequency one by one it is possible to see how good each approximation is by comparing to time simulations.

Here it will be shown that quite a lot of the HTM:s are diagonal, that is they only have a LTI part. Quantities as stator voltage, current and fluxes do have subdiagonals but when they are multiplied with each other to form power and torque the subdiagonals often cancels in this operating point. This phenomenon will be further commented in section 6.6.

Many calculations are made with and without PWM modelling. When not included the relation $e_s(t) = e_{s,sp}(t)$ is used. It could be seen as an inverter with infinte switching frequency.

The operating point of the engine and the parameters in this example is:

$$\psi_{\mu\alpha} = \cos 5\omega_0 t, \;\; \psi_{\mu\beta} = \sin 5\omega_0 t,$$

$$\psi_{r\alpha} = \cos\vartheta \cos(5\omega_0 t - \vartheta), \;\; \psi_{r\beta} = \cos\vartheta \sin(5\omega_0 t - \vartheta)$$

$$\lambda = 0, \;\; \omega_0 = 2\pi/0.25 \; rad\, s^{-1}, \;\; k_n = 0.3761, \;\; m_{sp} = 0.2, \;\; \vartheta = \frac{1}{2}\arcsin\frac{m_{sp}}{\gamma^2}$$

$$n_0 = 10.28, \;\; \rho = 1.05, \;\; \sigma = 0.06$$

$$V_m = 0.5, \;\; T_i = 0.05 \; s, \;\; \gamma = 1$$

$$U_{DC} = 1500 \; V, \;\; E^* = \frac{4}{\pi}1500 \; V, \;\; N = 75$$

6.3.1 HTM of $\Delta m_{is}(j\omega)/\Delta m_{sp}(j\omega)$

In figure 20 the HTM between the set point of the torque and the real value of the torque shown. For low frequencies the amplification is 1 which implies there is no constant error. For higher frequencies the changes are to fast for the system to completely respond to. That means the real torque will not oscillate with the same amplitude as the set point. That is good as these frequencies are high and the torque should not change so fast.

Some values taken from time simulations are plotted in the same figure and fits well to the models. For frequencies lower than 50 Hz there are very small disagreement between the results with and without PWM. For higher frequencies the PWM amplifies the amplitude and produces a larger time delay. Thus for frequencies larger than 50 Hz it is recommended to include $\mathcal{G}_{PWM}$ in the calculations.

The subdiagonals of the HTM are cancelled in this operating point. Therefore the relation is purely LTI, at least in a first order approximation. The time simulations confirm this.

By changing V_m and T_i it is possible to change the appearance of this curve. When T_i is increased the small amplitude peak by 15 Hz is moved to higher frequencies and becomes larger. By increasing V_m the curve is raised for frequenices < 100 Hz. To move the peak to the right and to maintain the size you should therefore increase T_i and decrease V_m.

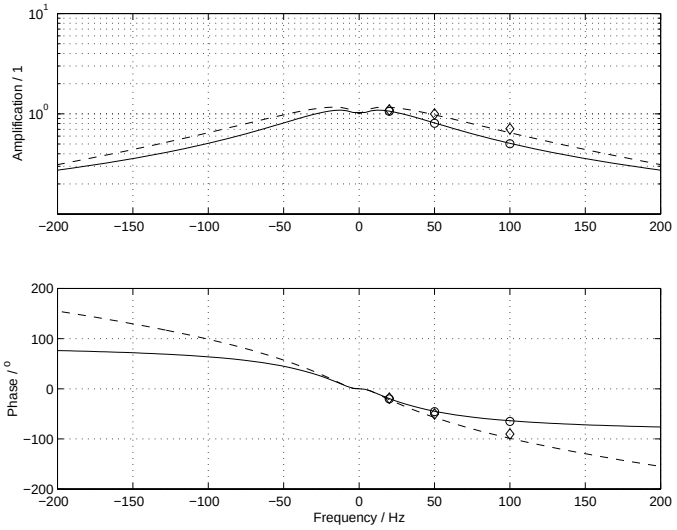

Figure 20: The main diagonal of the HTM between $\Delta m_{is}(j\omega)$ and $\Delta m_{sp}(j\omega)$, that is the Bode plot. The solid line comes from $\hat{G}$ with PWM modeling excluded, the PWM model is included in the dashed line. (◊) are from time simulations with PWM and (o) are from simulations without PWM.

6.3.2 HTM of $\Delta I_{DC}(j\omega)/\Delta m_{sp}(j\omega)$

Here the HTM to study the influence of m_{sp} on I_{DC} is constructed. In figure 21 the linear part (main diagonal) of the HTM is plotted. It appears to be a rescaled variant of figure 20. That makes sense because in this operating point the DC-link voltage is constant as well as the mechanical frequency. The mechanical power is proportional to the product of the torque and the mechanical frequency ($p_{mechanical} \sim k_n \times m_{is}$). And as I_{DC} is calculated from the total power this looks reasonable, the electrical losses don't change the appearance. The sidebands of the HTM, which could be caused from the electrical losses, cancels and reduces to a linear behavior. Time simulations confirm this.

Also in this case the similarity between the two models is large when $< 50\ Hz$.

6.3.3 HTM of $\Delta m_{is}(j\omega)/\Delta n(j\omega)$

If the mechanical frequency starts to change it is interesting to know if the controller is able to compensate for this and keep the torque constant. Figure 22 shows that the torque to a large extent really is constant. For higher frequencys the converter starts to influence and degrades the controller performance a bit, but the influence is small. $\mathcal{G}_{PWM}$ cathches the converter effects well, especially for frequencies larger than $50\ Hz$.

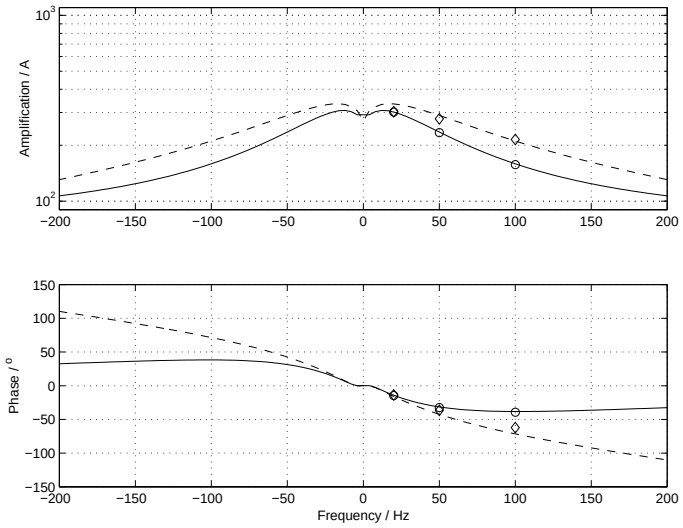

Figure 21: The main diagonal of the HTM between $\Delta I_{DC}(j\omega)$ and $\Delta m_{sp}(j\omega)$, that is the Bode plot. The solid line is from the HTM without PWM modeling and the dashed is with PWM modeling. The ($\Diamond$) are from time simulations with PWM and (o) without PWM. The solid line is from the model without PWM and the dashed one comes from the model with PWM.

6.3.4 HTM of $\Delta I_{DC}(j\omega)/\Delta n(j\omega)$

With the results from 6.3.3 we can expect that the power is almost purely linear dependent on the mechanical frequency when torque set point is constant, as mechanical power = mechanical frequency $\times$ torque. Figure 23 confirms this as the DC-link voltage is constant. The amplification is constant which looks reasonable with the power considerations in mind. A phase lag is though introduced due to the converter.

Here it turns out that the results with $\mathcal{G}_{PWM}$ becomes a bit unstable for low frequencies. In general if only the amplitude behavior is of interest it is recommended to exclude the PWM model.

6.3.5 HTM of $\Delta y_{\alpha}(j\omega)/\Delta m_{sp}(j\omega)$

At last we will see some nondiagonal HTM:s. Here the relationship between the torque set point and the stator current will be shown. All the calculations here are made without $\mathcal{G}_{PWM}$. In figure 24 the absolute values of the HTM is plotted in 3-D. If it is multiplied with an input vector with *one* frequency, that is containing two complex conjugated elements the output becomes *two* frequencies (four elements). From the look of the HTM it is seen that higher frequencies have less influence on the stator current.

In figure 25 time domain results are plotted over one fundamental period. The input is a pure cosine and in the output there are two frequencies - a non-LTI effect. When compared to time simulations it is seen that the low frequency parts are almost perfectly modeled. The high frequency ripple

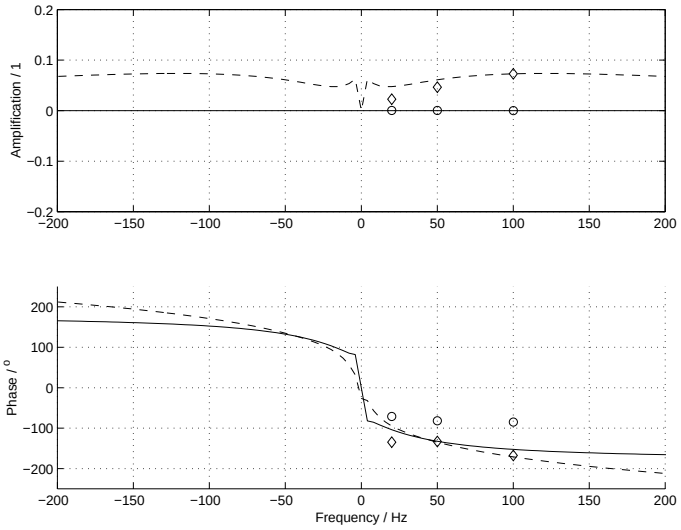

Figure 22: The main diagonal of the HTM between $\Delta m_{is}(j\omega)$ and $\Delta n(j\omega)$, that is the Bode plot. ($\Diamond$) are from time simulations with PWM and (o) without PWM.

from the converter is not captured with the HTM. The error is very small.

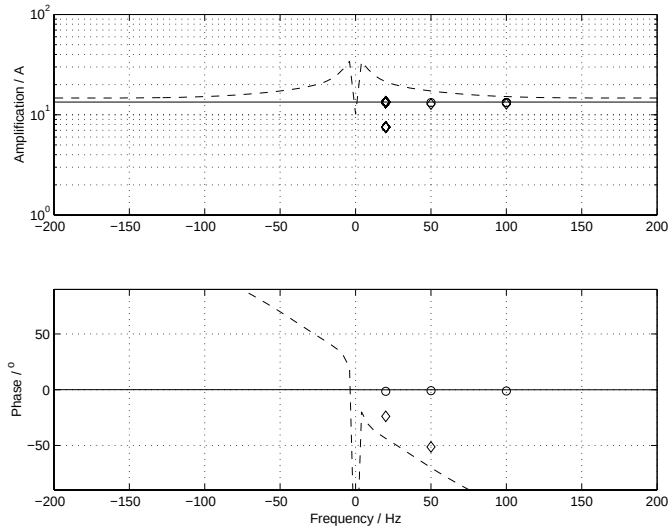

Figure 23: The main diagonal of the HTM between $\Delta I_{DC}(j\omega)$ and $\Delta n(j\omega)$, that is the Bode plot. The solid line comes from HTM without PWM modeling and the dashed with PWM modeling. ($\Diamond$) are from time simulations with PWM and (o) without PWM.

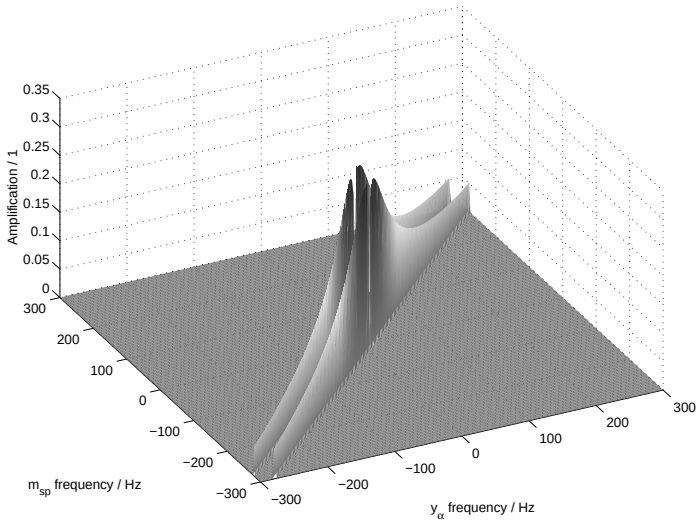

Figure 24: The absolute values of the HTM between $\Delta y_\alpha(j\omega)$ and $\Delta m_{sp}(j\omega)$. It contains two strong subdiagonals.

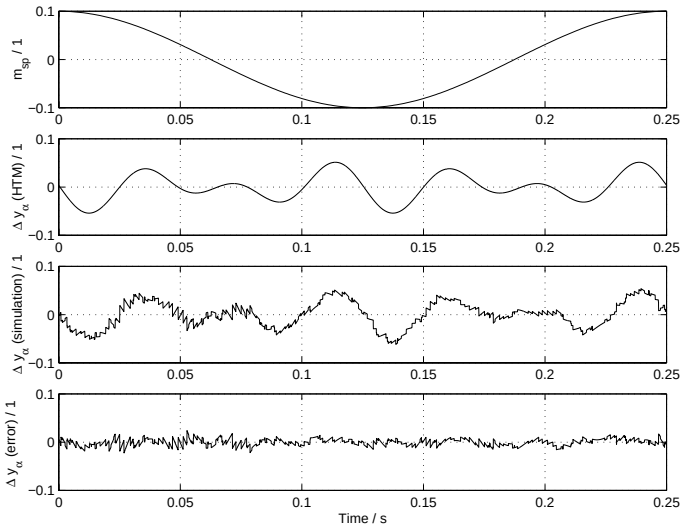

Figure 25: The time domain appearance over one fundamental period, T, of the normalized stator current Δy_α is plotted for the HTM and the time simulations with PWM. The absolute error is plotted in the last graph.

6.4 Test of Closed Loop with Mechanics

Here almost the same operating point as in 6.3 will be used. The difference is that the mechanical frequency is dependent on the torque. With the simple mechanics model there is an easy steady-state relation between the two.

First two Bode plots will made to see if the results fit well to time simulated values. We will also see if the PWM model is needed. Then the mechanical parameters are going to be changed and we will see what happens to the frequency response.

6.4.1 HTM of $\Delta n(j\omega)/\Delta m_{sp}(j\omega)$

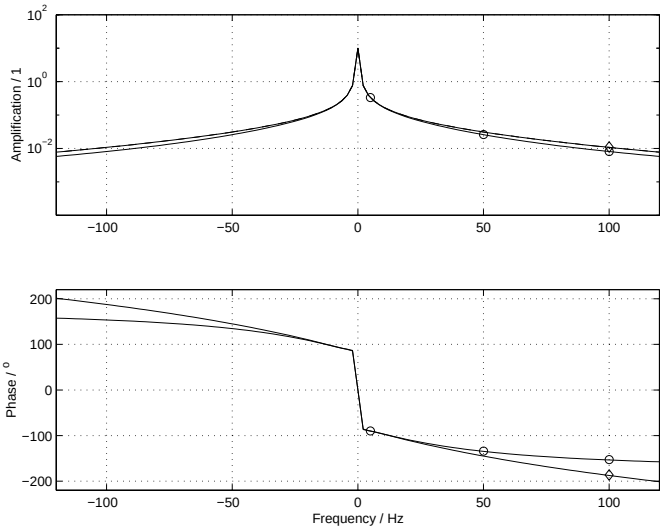

Figure 26: The mechanical response to torque changes: $\Delta n(j\omega)/\Delta m_{sp}(j\omega)$. The solid line comes from $\hat{G}$ without PWM modeling, in the dashed line is the PWM model included. ($\Diamond$) is a time domain result with PWM model and (o) are results without PWM.

Here the changes of the mechanical frequency due to torque set point changes are studied. $K_{train} = 0.1$ and $L = 0.1$ are used which means the system is stable by $n = 2$ ($k_n = 0.195$). A Bode plot is shown in figure 26. As can be seen the amplitude bahavior is almost identical for the to models. The phase show a difference by large frequencies which is confirmed by the measurements.

The frequency response is very similar to a Bode plot of eq.(37) which means the system follows the changes in m_{sp} very well.

6.4.2 HTM of $\Delta I_{DC}(j\omega)/\Delta m_{sp}(j\omega)$

Here the changes of the current in the DC-link is shown dependent on torque set point changes. The DC-link voltage level is supposed to be constant all the time. A Bode plot is shown in figure 27. The two models give different

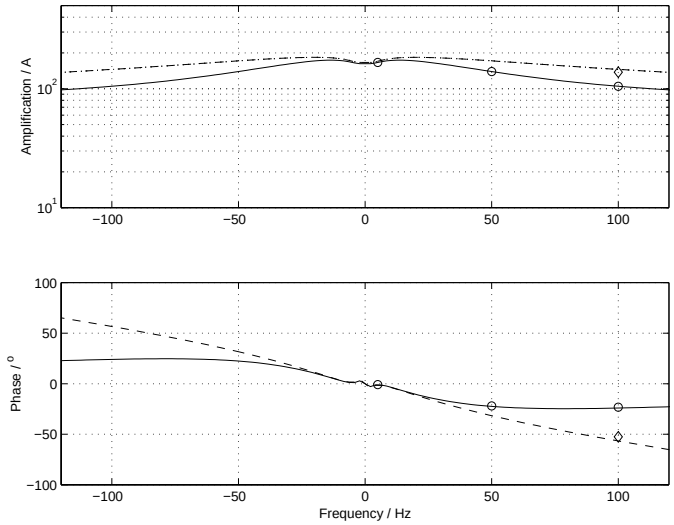

Figure 27: The DC-link current response to torque changes by constant DC-link voltage: $\Delta I_{DC}(j\omega)/\Delta m_{sp}(j\omega)$. The solid line comes from $\hat{G}$ without PWM modeling, in the dashed line is the PWM model included. ($\Diamond$) is a time domain result with PWM model and (o) are results without PWM.

results with frequencies larger than 50 Hz, just as in the modeling without mechanics. Here the mechanical frequency is a bit lower than in the former section but it still seems as 50 Hz is good breakpoint. As a rule of thumb the PWM model should be included when the operating point mechanical frequency is high and/or when the perturbation frequency is high (>50 Hz).

6.4.3 Change of the Mass

Here the same kind of plots will be made but the moment of inertia of the train is going to be changed. All the plots here are made without PWM modeling for clarity.

First of all the mechanical interaction is studied for different inertias, see figure 28. The results are quite intuitive: Smaller mass leads to larger response to torque changes, the curve blows up when the inertia is decreased. The relation is almost identical to a Bode plot of eq.(37) for low frequencies.

In figure 29 the DC-link current change for constant DC-link voltage level is plotted. It is seen that for high inertias ($K_{train} > 0.1$) the amplitude plots look almost identical. That is reasonable when you consider the mechanical energy, the product of the mechanical frequency and the torque. For high masses the response to a torque change is very small. The power is then only dependent on the torque change. For lower inertias though the mechanical frequency change is so large that the power is influenced, as is clearly seen in the plot.

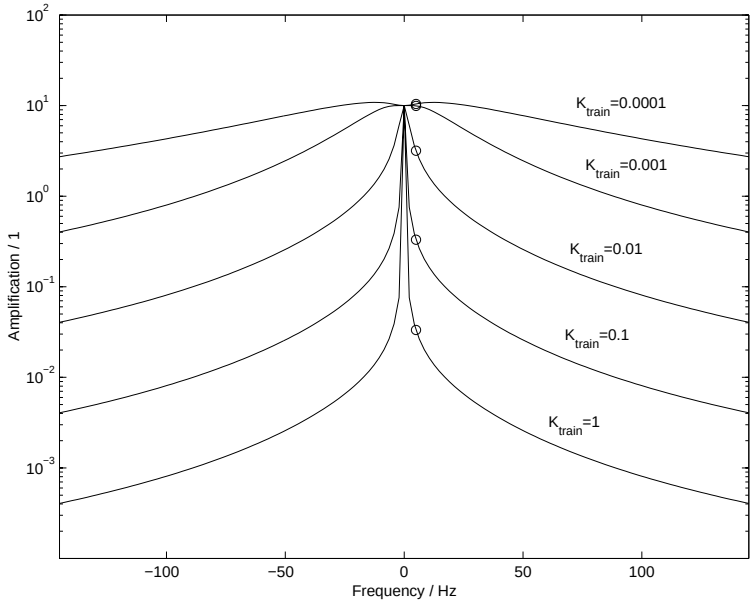

Figure 28: $\Delta n(j\omega)/\Delta m_{sp}(j\omega)$ for variable moment of inertia. (o) are values from time simulations.

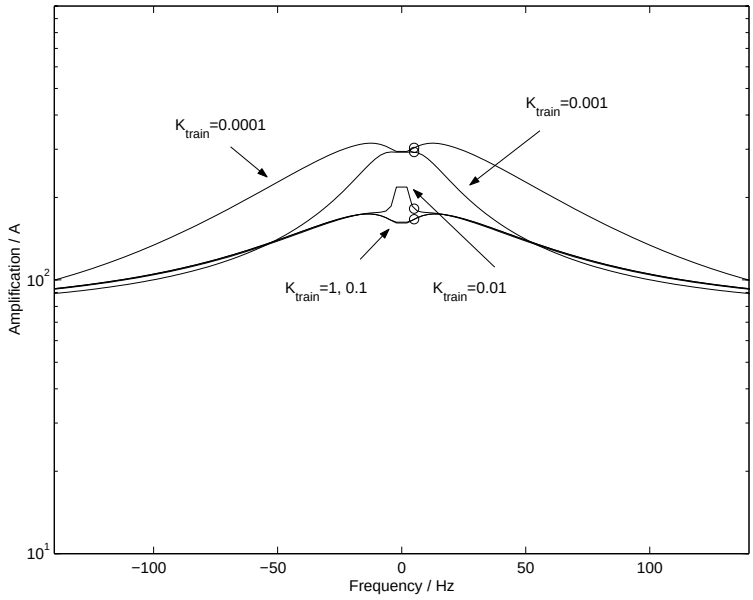

Figure 29: $\Delta I_{DC}(j\omega)/\Delta m_{sp}(j\omega)$ is plotted for different inertias.

6.4.4 Change of the Friction

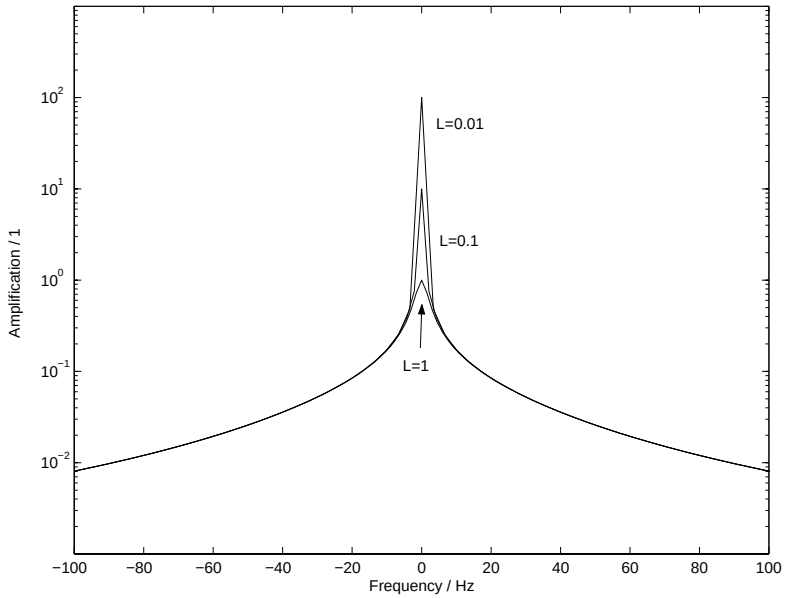

Figure 30: $\Delta n(j\omega)/\Delta m_{sp}(j\omega)$ is plotted for different friction coefficients.

Here the friction coefficient is going to be altered. The operating point value of the mechanical frequency is dependent on the friction. If the friction is decreased the steady-state frequency is increased. Here the friction is decreased as far as to $L = 0.001$ which means n stabilize around 200 when $m_{sp} = 0.2$. Such high frequencies are not used in reality and definitely not with indirect self control. So these cases are more academic.

In figure 30 the mechanical response is shown. The only differenc here is by very low frequencies. That is reasonable when you study eq.(37). L comes in as a constant in the denominator. For high ω it is negliable and doesn't influence much.

In figure 31 the DC-link current behavior for constant DC-link voltage ($1500\ V$) is plotted for different values of the friction. The appearance of the curves don't change much as to a constant offset. The reason is that each curve has an operating point frequency that differs with a factor of ten. A higher frequency lifts the curve accordnig to the discussion with mechanical energy. For small L the change is almost a factor of 10. For higher L the change is not so large which is explained with the constant L in the denominator of eq.(37).

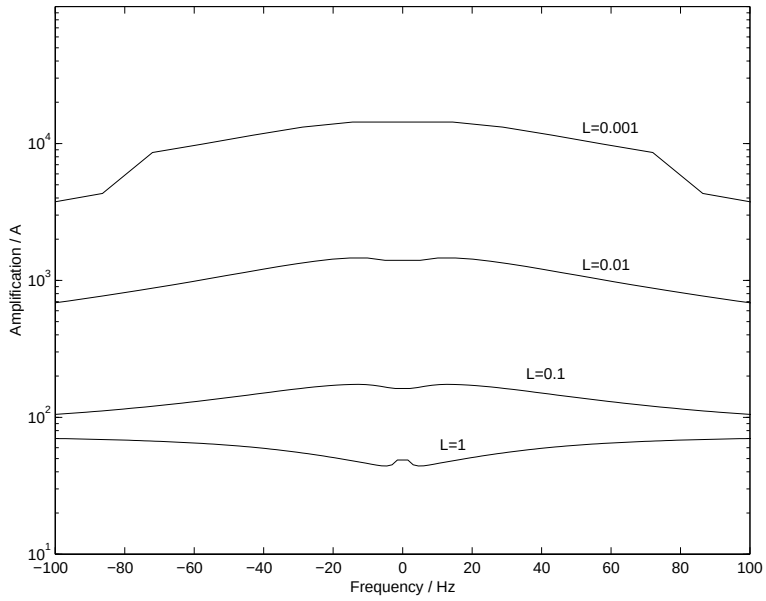

Figure 31: $\Delta I_{DC}(j\omega)/\Delta m_{sp}(j\omega)$ is plotted for different friction coefficients. (o) are time simulated values.

6.5 DC-link Interaction

Here we will se how the motor side interact with the DC-link. Until now the DC-link has been considered to have a constant voltage. What happens when it starts to oscillate? In the converter modeling the assumption was made that the PWM compensated for these variations. How good this assumption was will be shown through an example.

One of the goals of this work was to calculate an admittance matrix. Here it will be done and the effect of the torque compensator, eq.(41), will be shown. The scheme presented to obtain an operating point will be followed in order to do this.

6.5.1 Effects of Oscillating DC-link Voltage

Here the same operating point as in 6.4.1 will be used with one exception:

$$U_{DC} = 1500 + 300 \sin 2\pi 33\, t \ V$$

That is the DC-link voltage oscillates with 33 Hz with an amplitude of 20% of the DC component. As DC oscillation effects were neglected in the modeling exact the same matrices as in 6.4.1 are used. Then some `Simulink` tests are made to see if the effects really are negliable. As perturbation is

$$\Delta m_{sp} = 0.2 \cos \omega t$$

used. With $\omega = 2\pi 10$ and $2\pi 50$ $rad\, s^{-1}$. The results are given in table 3.

Quantity	10 Hz	50 Hz
$\delta m_{is}/\delta m_{sp}$	$1.10\angle -7.20°$	$0.968\angle -52.8°$
$\delta p/3000\delta m_{sp}$	$174\angle -3.30°$	$162\angle -29.5°$
$\delta n/\delta m_{sp}$	$0.174\angle -96.3°$	$0.0308\angle -143°$

Table 3: Measurement data from simulation with oscillating DC-link voltage. The amplification and the phase lag is given for each quantity.

These measurements can be compared to the results presented in figure 26 and 27. There is a good agreement. That is also the case for the torque measurement although no figure is included in the report.

Although there is a large variation in the DC-link voltage, the PWM compensates very well and eliminate the effects. Some other tests were also performed and it turns out that the effects are negliable or very small for DC-link variations < 100 Hz (switching frequency 250 Hz). *Thus the assumption of neglecting the effects of DC-link variations on the motor is very good under these circumstances.*

6.5.2 Calculation of Admittance Matrix and Operating Point

To calculate the admittance matrix and the operating point you first have to decide a DC-link voltage spectrum. The problem is then to find the DC-link current spectrum and the motor states. When eq.(41) is excluded it is easy: the linear equation system (42) is solved and then power balance is used

to compute the admittance matrix. The engine side works as a negative resistor.

To stabilize the link eq.(41) is used. An example will be carried through to show how the computations are done. As DC-link voltage is

$$U_{DC}(t) = 1500 + 300\sin\omega t\ V,\ \ \omega = 2\pi 33\ rad\,s^{-1},\ \ U_{DC,sp} = 1500\,V$$

chosen. The motor controller is given the set point: $m_{sp} = 0.2$. This set point is modified through (41). The result is:

$$m_{sp,new} = 0.204 + 0.08\sin\omega t - 0.004\cos 2\omega$$

The constant part, 0.204, is used as operating point for the engine and the motor matrix, $\hat{\mathcal{G}}$, is calculated as before. The constant part of the needed power is given in that process. The oscillating power components are given with the help of $\mathcal{G}_p$ with [1]

$$\Delta m_{sp} = 0.08\sin\omega t - 0.004\cos 2\omega t$$

Now the total power is known. (42) is used to get the operating point DC-current spectrum:

$$I_{DC}(t) = 60.0 - 10.5\cos\omega t + 15.6\sin\omega t + 0.549\cos 2\omega t + 0.191\sin 2\omega t\ A$$

The admittance matrix is given by eq.(40). $\mathcal{U}_{ref}$ is coupled to $\Delta\mathcal{U}_{DC}$. This coupling is included by an approximation of (41):

$$\Delta m_{sp,new}(t) = \frac{2U_{DC}(t)m_{sp}}{U_{DC,sp}^2}\Delta U_{DC}(t)$$

As it is a convolution the transformation to frequency domain is made according to 2.4.1. Let's call this HTM $\mathcal{G}_C$. The admittance matrix is then

$$\mathcal{G}_{ad} = \mathcal{U}_{DC}^{-1}\left[\frac{1}{2}\mathcal{G}_p\mathcal{G}_C - I_{DC}\right] \tag{43}$$

The absolute values of the admittance matrix are plotted in figure 32. It is seen that the main diagonal by far is dominating. Two sidebands can be seen with the frequency shifts $\pm\omega$ and $\pm 2\omega$. The Bode plot of the main diagonal is given in figure 33. Especially the phase plot is of interest: it is seen that the phase lag is less than 90° for frequencies <50 Hz. That is a large improvement compared to when the DC-compensator is excluded. Then the phase lag is 180° for all frequencies, as the motor side works as a negative resistor. Now the motor side works as a normal resistor in series with an inductor for frequencies <50 Hz. The admittance converges to 0.06 A/V when the frequency is higher than 300 Hz. The phase lag is then about 180°.

[1] An interpolation of $\mathcal{G}_p$ must be performed when the frequency components of $\Delta m_{sp,new}$ are not parts of the motor side frequency basis. When $\mathcal{G}_p$ is purely diagonal a simple linear interpolation is made along the diagonal. Non-diagonal elements can be interpolated with for example bilinear or spline methods. The effects of such off-diagonal interpolation is *not* investigated here.

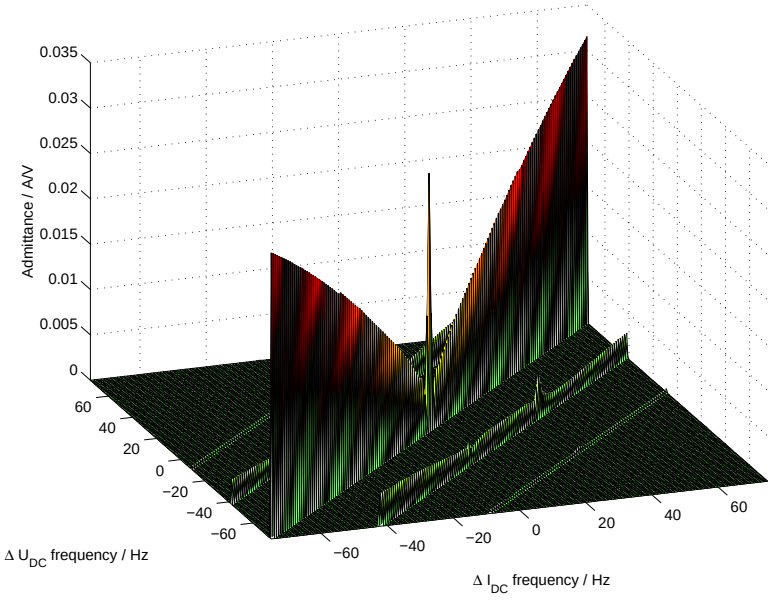

Figure 32: The admittance matrix for the motor side. Two small sidebands can be seen. The peak in the middle is a result of the approximation.

For very low frequencies there is a peak. This is a result of the approximations. The motor is linearized with a fundamental frequency, ω_s. All results are described in multiples of this frequency. When the constant part of the DC-link voltage ($0\ Hz$) is raised the constant part of the torque set point is increased. This leads to a higher ω_s. Thus the operating point is no longer valid. *The results here may not be used for constant changes of the DC-link! If a constant change is to be studied the motor side has to be relinearized.*

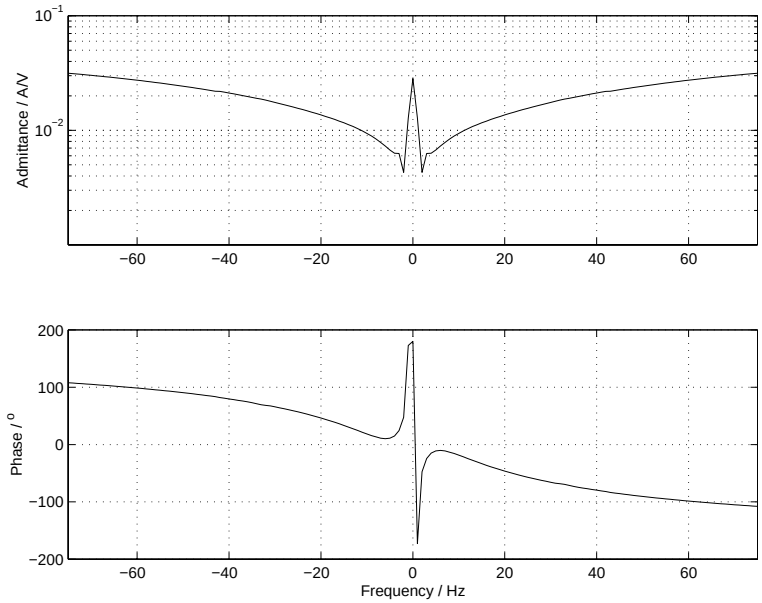

Figure 33: The Bode plot of the admittance matrix. The results by 0 Hz are not valid according to the discussion in section 6.5.2.

6.6 Comment on the Spectrum of the Power

In the tests made it turned out that the power and torque HTM:s ended up having only diagonal parts. This may seem strange as the voltage, current and flux matrices do have non-diagonal elements. The reason for this is the choice of operating point: the total flux moving on a circle. This total symmetry leads to elimination of the subdiagonals. That is also the reason the motor delivers constant torque and needs constant power in the operatng point.

If we for example consider the power, we get the following results. Let the operating point stator voltage be:

$$u_\alpha = A\,\cos(\omega t + \alpha),\;\; u_\beta = A\,\sin(\omega t + \alpha)$$

and the corresponding stator current

$$y_\alpha = B\cos(\omega t + \beta),\;\; y_\beta = B\sin(\omega t + \beta)$$

If any perturbation is introduced the controller amplitude and phase modulates the voltage. This leads to amplitude and phase modulation of the current as well. Thus A, B, α and β become time dependent. The motor power is expressed as:

$$p_{motor} \sim u_\alpha y_\alpha + u_\beta y_\beta$$

With some trigonometric transformation this can be simplified to:

$$p_{motor} \sim A(t)B(t)\cos[\alpha(t) - \beta(t)]$$

Thus the power is independent of the electrical frequency ω. When this power expression is approximated it leads to a diagonal matrix.

Notice that when the operating point voltages are a bit unsymmetric or/and contain higher harmonics, the power is dependent on ω. Thus if the flux is controlled on a hexagon the power will have time dependet components and the power matrix will have non-zero subdiagonals.

7 Conclusions

As can be seen it is possible to model an AC-locomotive with the help of truncated Fourier series. The frequency interaction turned out to be quite limited when the total flux is controlled on a circle. That is in fact a good thing because then you now what frequencies are created in the system. If an input frequency generates a lot of other frequencies there is a risk that one them excite a resonance state in the mechanics or in the DC-link. When the total flux is controlled on a hexagon, as is the case for higher speeds, the frequency interaction is larger.

The constructed HTM of the system, $\hat{G}$, turned out to give results that fitted very well to the results from time simulations. The effects of the PWM controlled converter turned out to be negliable for perturbations with frequency less than 50 Hz. But as the mechanical frequency increases the modeling of the PWM becomes more important as the applied stator voltage spectrum then less resembles the wanted one. Thus it is recommended to include the PWM model for high frequency perturbations. In general the effects of the PWM led to an increased time lag and an amplitude amplification for high frequencies.

The mechanical model was very simple but provided a relation between the torque and the mechanical frequency. The mass of the system is an important parameter. When studying the DC-link effects, high mass systems show a similar behaviour to one another. When the mass is decreased the mechanical frequency starts to be more influenced and therefore the DC-link interaction changes. The friction parameter only has an influence for low frequencies according to the results here.

With power balance an admittance matrix of the motor side was computed. Two different cases were treated: with and without DC-link compensator. Without the compensator the motor side works as a negative resistor because of the PWM controlled converter. The PWM adjusts the switching signals when the DC-link voltage changes so that hardly no changes can be seen on the motor side. Thus a voltage *increase* leads to a current *decrease*. This behaviour might inflict stability problems. Therefore the compensator is implemented. The results showed that with the compensator the motor side works as a passive component for voltage changes under 50 Hz. The stability of the DC-link should therefore be better with the compensator.

The admittace matrix was strongly diagonal dominant. The small side bands are created from the DC-link voltage spectrum. When the total flux of the motor is controlled on a hexagon other sidebands appear with frequency change of multiples of the electrical frequency. This is an unwanted effect. A way to reduce these effects would be to control the flux on a shape that more resembles a circle.

An iterative scheme was presented that could be used to connect the model to a line side model. First the user has to give a DC-link voltage spectrum and a set point for the torque. Then it is possible to compute the DC-link current spectrum and an admittance matrix. The current spectrum then is given to a similar line model which in turn gives a new voltage spectrum. The scheme is repeated until convergence.

7.1 Future Work

The next steps would be to make similar models for the other two controllers, the DSC-TB and the FW-DSC. The motor and the converter model presented here could be used. Thus the work would be to find new matrices $\mathcal{E}$ and $\mathcal{F}$. A new operation point must then be used. The flux moving on a hexagon is a natural choice.

The connection with the line side model is also an interesting issue. Then you could answer questions like: what effects have perturbations in the mechanical frequency on the railway net current?

The mechanical model used in this work was quite primitive. A more complicated and realistic model would be interesting to use. Then the effects of mechanical resonances on the DC-link could be studied.

The connection between the DC-link and the motor side was made with power balance. It is also possible to use a more direct method with the converter model, $S(t)U_{DC}(t)$ directly. Then the spectrum of $S(t)$ must be modeled. By using the techniques presented in Appendix A this is possible. By using Kirchoff's laws the currents can also be calculated if $S(t)$ is known.

The computations can be carried out in a rotating coordinate system. Some effects are then easier to model, the flux control for example.

The equations here end up in a linear equation system. It is quite sparse with a main diagonal and some subdiagonals. To use Gaussian elimination to solve such systems often is inefficient. Equation system of this type can often be solved with iterative methods like Gauss-Seidel. Then computation time would be saved and larger frequency vectors could be used. As comparison needs Gaussian elimination $O(N^3)$ operations while Gauss-Seidel needs $O(N)$.

8 Bibliography

References

[1] Möllerstedt, E. (1998): *An Aggregated Approach to Harmonic Modelling of Loads in Power Distribution Networks*. Lic thesis ISRN LUTFD2/TFRT-3221–SE, Department of Automatic Control, Lund Institute of Technology, Box 118, S-221 00 Lund, Sweden

[2] Wereley, N.M. (1990): *Analysis and Control of Linear Periodically Time Varying Systems*. PhD thesis, Department of Aeronautics and Astronautics, Massachusetts Institute of Technology, Cambridge, Massachusetts 02139, U.S.A.

[3] Meyer, M. (1999): "Netzstabilität in grossen Bahnnetzen", *Schweizer Eisenbahn-Revue*, 7-8/1999, pp. 312-317, Switzerland

[4] Gilmore, R.J. and M.B. Steer (1991): "Nonlinear Circuit Analysis Using the Method of Harmonic Balance - A Review of the Art. Part I. Introductory concepts." *Int J. Microwave and Millimeter-Wave Computer-Aided Eng.*, 1:1, pp. 22-37.

[5] Spanne, S. (1982): *Föreläsningar i Funktionsteori*, Mathematics Department, Lund Institute of Technology, Sweden

[6] Nilsson, J.W. and S.A. Riedel (1996): *Electric Circuits*, Fifth edition, ISBN 0-201-40100-2, Addison-Wesley Publishing Company

[7] Olsson, H. (1998): *An Approach to Frequency Domain Network Computations Allowing Description of Nonlinearities* Technical report, Daimler-Benz, Berlin, Germany

[8] Meyer, M. (1990): "Über das Netzverhalten von Umrichterlokomotiven", *Schweizer Eisenbahn-Revue*, 8-9/1990, Switzerland

[9] Filipović, Ž. (1989): *Elektrische Bahnen*, ISBN 0-387-51121-0, Springer-Verlag

[10] Menth, S. and S. Schmidt (1997): *Modeling of Traction Motor Control Schemes in Matlab/Simulink*. Technical report, ABB CHCRC 97-34, ABB Corporate Research Center Baden, CH-5405 Baden-Dättwil, Switzerland

[11] McPherson, G. and R.D. Laramore (1990): *An Introduction to Electrical Machines and Transformers*, Second edition, ISBN 0-471-63529-4, John Wiley & Sons

A HTM of Pulse Width Modulation

Here the HTM used in section 5.1 is going to be derived. Let the output rectangle wave be $u(t)$ and the input reference wave of period T be $v(t)$. $u(t)$ has the values $\pm E$ and in order to be T-periodic $T/2T_p$ must be an integer. Call this integer N. The triangle carrier wave is chosen to have the value $+E$ at $t = 0$.

In the following the real representation of the Fourier series will be used:

$$v(t) = \sum_{k=0}^{\infty} a_k \cos k\omega_0 t + b_k \sin k\omega_0 t, \quad \omega_0 = \frac{2\pi}{T}$$

and the function is represented with the vector

$$\mathcal{V} = (\ a_0\ a_1\ b_1\ a_2\ b_2 \dots\ )^T$$

The series is truncated after Q frequencies.

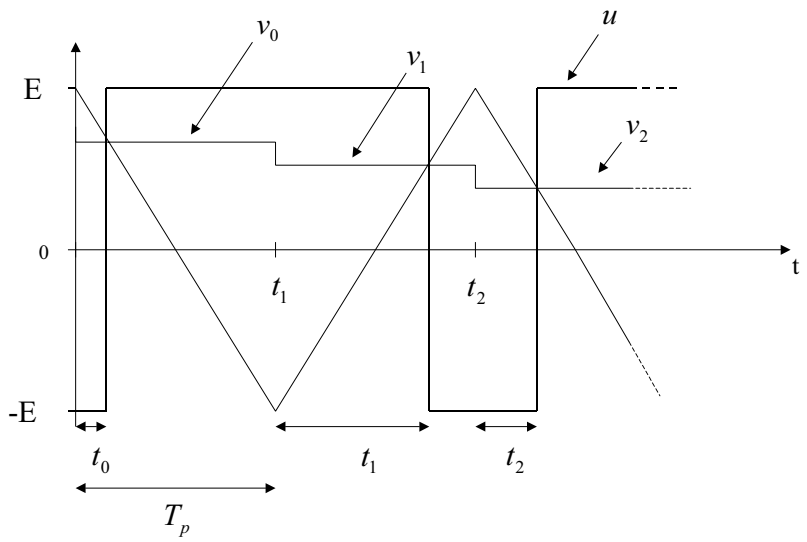

Figure 34: The PWM method with some new variables introduced.

First of all an input function $v(t)$ with spectrum $\mathcal{V}$ is chosen as operating point. It has the values v_i in t_i, $i \in [0, 1, 2, \dots, 2N-1]$. The correspondig output is $u(t)$ with spectrum $\mathcal{U}$ and has the values E_i in t_i. N.B. $E_i = -(-1)^i E$.

In order to get the output $u(t)$, the switching time points Δt_i have to be known. They easy to calculate according to figure 34 for a specific $v(t)$. A direct (approximative) relationsship between the input and the output spectrum differences is preferable, or in HTM formulation:

$$\delta\mathcal{U} = \mathcal{G}_{PWM}\ \delta\mathcal{V} \tag{44}$$

$$\delta\mathcal{U} = (\ \delta A_0\ \delta A_1\ \delta B_1 \dots\ )^T \quad \delta\mathcal{V} = (\ \delta a_0\ \delta a_1\ \delta b_1 \dots\ )^T$$

In order to get a HTM let's calculate what happens with v_i when a perturbation $\delta\mathcal{V}$ is introduced. According to the Fourier series the change is:

$$\delta v_i = \sum_{k=0}^{Q} \delta a_k \cos k\omega_0 t_i + \delta b_k \sin k\omega_0 t_i$$

This can be written in matrix form:

$$\begin{pmatrix} \delta v_0 \\ \delta v_1 \\ \vdots \\ \delta v_{2N-1} \end{pmatrix} =$$

$$\begin{pmatrix} 1 & \cos\omega_0 t_0 & \sin\omega_0 t_0 & \dots & \sin Q\omega_0 t_0 \\ 1 & \cos\omega_0 t_1 & \sin\omega_0 t_1 & \dots & \sin Q\omega_0 t_1 \\ \vdots & \vdots & \vdots & \ddots & \vdots \\ 1 & \cos\omega_0 t_{2N-1} & \sin\omega_0 t_{2N-1} & \dots & \sin Q\omega_0 t_{2N-1} \end{pmatrix} \begin{pmatrix} \delta a_0 \\ \delta a_1 \\ \delta b_1 \\ \vdots \\ \delta b_Q \end{pmatrix}$$

If the changes in v_i are known the changes in Δt_i, δt_i, can be calculated as

$$\delta t_i = \frac{T_p}{2E_i}\delta v_i$$

Now we have a relation between $\delta\mathcal{V}$ and the changes in the switching time points, δt. In matrix form we write:

$$\delta t = \mathcal{G}_1 \, \delta\mathcal{V} \tag{45}$$

The next step is to see how the output spectrum depends on the switching points Δt_i. The Fourier coefficients $\mathcal{U}$ of the output can be calculated when Δt_i are known. The coefficients are defined as:

$$A_0 = \frac{1}{T}\int_0^T u(t)\,dt, \;\; A_k = \frac{2}{T}\int_0^T u(t)\cos k\omega_0 t\,dt, \;\; B_k = \frac{2}{T}\int_0^T u(t)\sin k\omega_0 t\,dt$$

As the output is known to be a square signal of values $\pm E$ the coefficients can be written as:

$$k \neq 0: \;\; A_k = \frac{2}{T}\sum_{i=0}^{2N-1}\int_{iT_p}^{(i+1)T_p} u(t)\cos k\omega_0 t\,dt =$$

$$\frac{2}{T}\sum_{i=0}^{2N-1}\left\{E_i\left[\frac{\sin k\omega_0 t}{k\omega_0}\right]_{iT_p}^{iT_p+\Delta t_i} + E_{i+1}\left[\frac{\sin k\omega_0 t}{k\omega_0}\right]_{iT_p+\Delta t_i}^{(i+1)T_p}\right\} \overset{[E_{i+1}=-E_i]}{=}$$

$$\frac{2}{T}\sum_{i=0}^{2N-1} E_i\left\{\frac{2\sin k\omega_0(iT_p+\Delta t_i)}{k\omega_0} - \frac{\sin k\omega_0 iT_p + \sin k\omega_0(i+1)T_p}{k\omega_0}\right\} \tag{46}$$

B_k can analogously be written as:

$$B_k = \frac{2}{T}\sum_{i=0}^{2N-1}\int_{iT_p}^{(i+1)T_p} u(t)\sin k\omega_0 t\,dt =$$

$$\frac{2}{T}\sum_{i=0}^{2N-1} E_i \left\{ -\frac{2\cos k\omega_0(iT_p+\Delta t_i)}{k\omega_0} + \frac{\cos k\omega_0 iT_p + \cos k\omega_0(i+1)T_p}{k\omega_0} \right\} \quad (47)$$

To see how the changes of Δt_i influence $\mathcal{U}$ lets differentiate the coefficients (46) and (47) with respect to Δt_i. The results for small δt_i are

$$\delta A_k = \frac{4}{T}\sum_{i=0}^{2N-1} E_i \cos k\omega_0(iT_p+\Delta t_i)\delta t_i, \;\; K \neq 0$$

$$\delta B_k = \frac{4}{T}\sum_{i=0}^{2N-1} E_i \sin k\omega_0(iT_p+\Delta t_i)\delta t_i$$

or in matrix form:

$$\begin{pmatrix} \delta A_0 \\ \delta A_1 \\ \delta B_1 \\ \vdots \\ \delta B_Q \end{pmatrix} =$$

$$\frac{4}{T}\begin{pmatrix} E_0/2 & E_1/2 & \dots & E_{2N-1}/2 \\ E_0\cos\omega_0\tau_0 & E_1\cos\omega_0\tau_1 & \dots & E_{2N-1}\cos\omega_0\tau_{2N-1} \\ E_0\sin\omega_0\tau_0 & E_1\sin\omega_0\tau_1 & \dots & E_{2N-1}\sin\omega_0\tau_{2N-1} \\ \vdots & \vdots & \ddots & \vdots \\ E_0\sin Q\omega_0\tau_0 & E_1\sin Q\omega_0\tau_1 & \dots & E_{2N-1}\sin Q\omega_0\tau_{2N-1}) \end{pmatrix} \begin{pmatrix} \delta t_0 \\ \delta t_1 \\ \vdots \\ \delta t_{2N-1} \end{pmatrix}$$

where $\tau_j = jT_p + \Delta t_j$. Thus

$$\delta\mathcal{U} = \mathcal{G}_2\,\delta t \quad (48)$$

To get $\mathcal{G}_{PWM}$ in (44) we simply combine (45) and (48) and eliminate δt:

$$\mathcal{G}_{PWM} = \mathcal{G}_2\mathcal{G}_1 \quad (49)$$

□

A.1 Error Analysis

It is possible to carry out an error analysis of the results from $\mathcal{G}_{PWM}$. The errors come in the second part where differentiations of A_k and B_k are done. Thus the Fourier coefficients of the output is approximated with a Taylor sum of the first order. A Taylor expansion with three terms of a function f which is twice differentiable can be written

$$f(x+\delta x) = f(x) + f'(x)\delta x + \underbrace{\frac{f''(h)}{2}\delta x^2}_{R(h,\delta x)}, \;\; h \in]x, x+\delta x[$$

where $R(h,\delta x)$ is the error of the linear approximation.

If the expressions for A_k and B_k are studied it is possible to get the error $R(h,\delta t)$ for the whole sum:

$$R_{A,k}(h,\delta t) = \frac{2}{T}\sum_{i=0}^{2N-1} -E_i k\omega_0 \sin\left[k\omega_0(iT_p+\Delta t_i+h_i)\right]\delta t_i^2$$

$$R_{B,k}(h,\delta t) = \frac{2}{T}\sum_{i=0}^{2N-1} E_i k\omega_0 \cos\left[k\omega_0(iT_p + \Delta t_i + h_i)\right]\delta t_i^2$$
$$h_i \in]\Delta t_i, \Delta t_i + \delta t_i[$$

As sinusoidals only take values between -1 and $+1$ it is possible to make the following restrictions:

$$|R_{A,B,k}(h,\delta t)| \leq \frac{2|E|k\omega_0}{T}\sum_{i=0}^{2N-1}|\delta t_i|^2 \leq \frac{2|E_0|k\omega_0}{T}2N||\delta t||_\infty^2$$

It is also possible to make an upper bound of $||\delta t||_\infty$. From eq.(45) and the definition of matrix norms you get:

$$||\delta t||_\infty \leq ||\mathcal{G}_1||_\infty \, ||\delta\mathcal{V}||_\infty$$

When the expressions are combined we get the absolute upper bound of the error of a coefficient:

$$|R_{A,B,k}(h,\delta t)| \leq \frac{4|E_0|Nk\omega_0}{T}||\mathcal{G}_1||_\infty^2 \, ||\delta\mathcal{V}||_\infty^2 \tag{50}$$

As $\mathcal{G}_{PWM}$ ideally is an identity matrix the largest output Fourier coefficient should be of the same size as the input coefficients. When $R_{A,B,k}(h)$ starts to have this magnitude the results from the HTM are bad. Thus a criteria for using the HTM might be:

$$\frac{8\pi|E_0|Nk}{T^2}||\mathcal{G}_1||_\infty^2 \, ||\delta\mathcal{V}||_\infty^2 \leq \mu||\delta\mathcal{V}||_\infty$$

where μ is a ratio paramater for how large the errors may be. Notice that this error analysis is very pessimistic so higher values of k and $||\delta\mathcal{V}||_\infty$ might be ok to use.

B Documentation of MATLAB-Functions